

SCHOOL ON SYNCHROTRON RADIATION AND APPLICATIONS
In memory of J.C. Fuggle & L. Fonda

19 April - 21 May 2004

Miramare - Trieste, Italy

1561/11

Optical components for hard x-ray beamlines

Edoardo Busetto

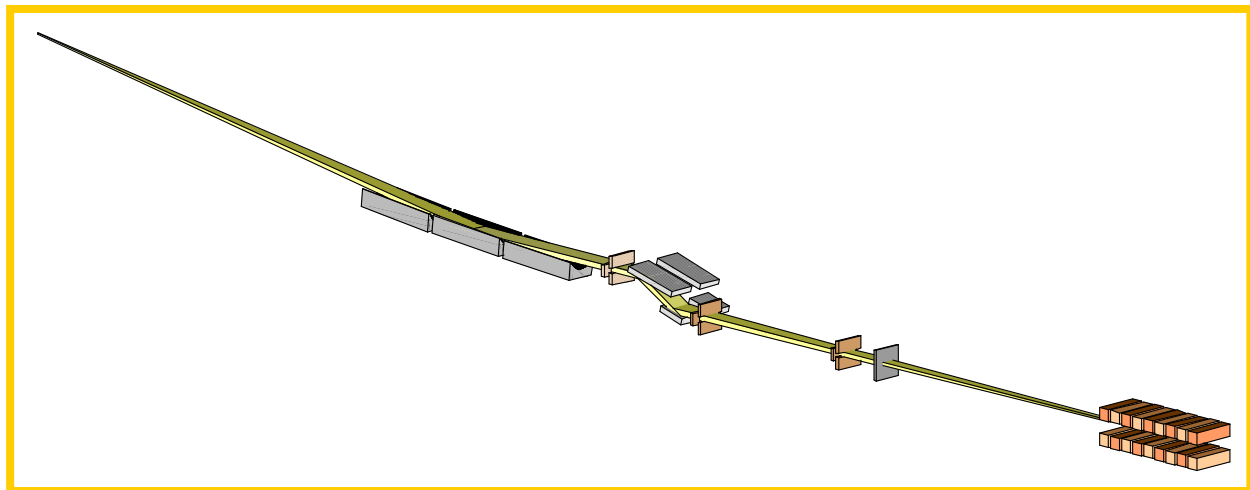
abdus salam
international centre for theoretical physics

School on Synchrotron Radiation

27 -28 April 2004

Optical components for hard x-ray beamlines

Edoardo Busetto



Sincrotrone Trieste S.c.p.A.
Hard-X Ray Optics
Laboratory

Optical components for hard x-ray beamline

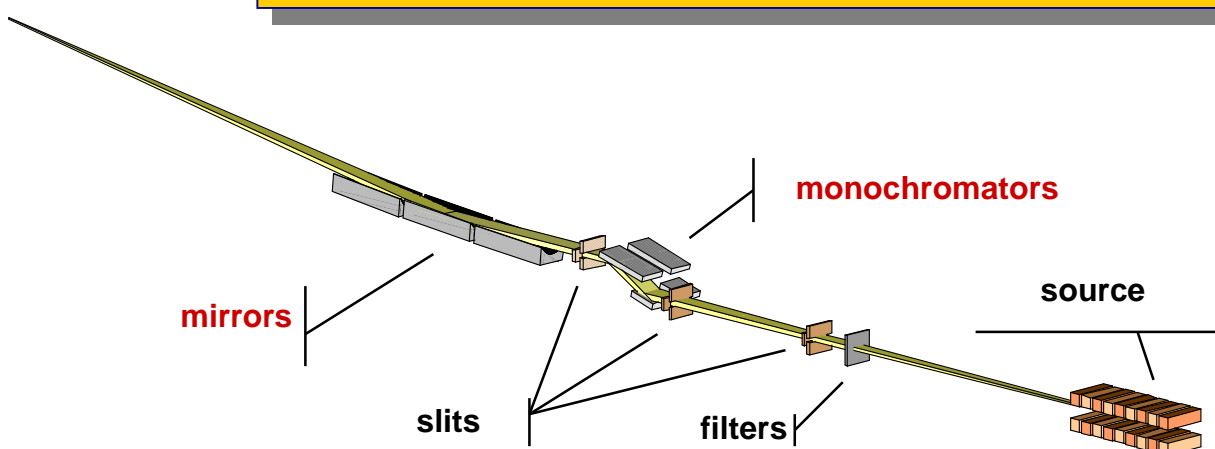
High brilliance and small electron beam emittance mean X-ray beams of high quality

“ ...The finite quality and the fundamental limits of the optical components increase the emittance of the beam.....

The main aim of the optical design consists on minimizing the inevitable beam degradation .”

Jean Sushko "Design parameters for hard x-ray mirrors: the ESRF case"
OPTICAL ENGINEERING/February 1995/Vol. 34 2/361

detectors



Most important optical elements:

- sources
- filters
- slits and pinholes
- **mirrors**
- **monochromators**
- **detectors**

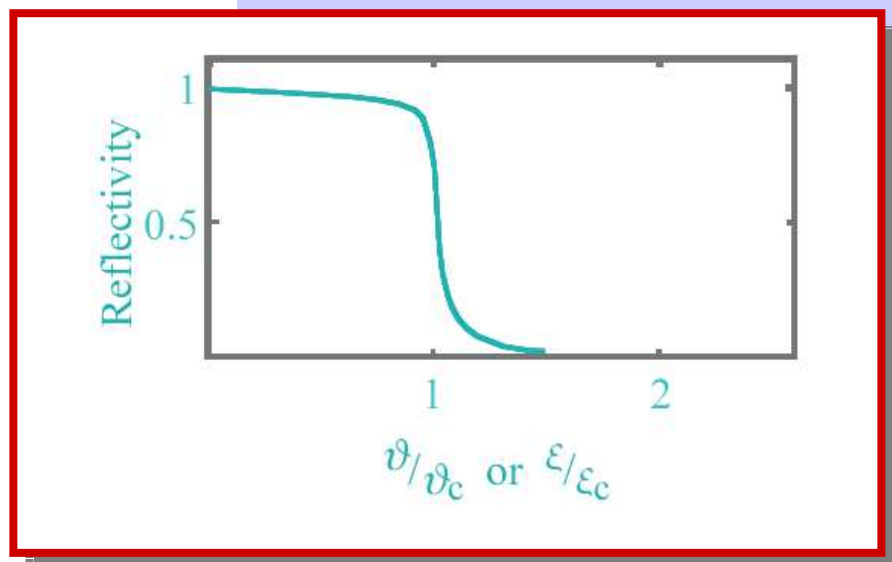


Sincrotrone Trieste S.c.p.A.
Hard-X Ray Optics
Laboratory

Mirrors 1: total reflection

For x-rays the refractive index is $n = 1 - \delta$
with $0 < \delta \ll 1$, therefore is $0 < n < 1$

If we consider ϑ as the angle that the incoming radiation does with the mirror surface (*grazing angle*), the photons will be totally reflected if $\vartheta < \vartheta_c$



$$\vartheta < \vartheta_c$$

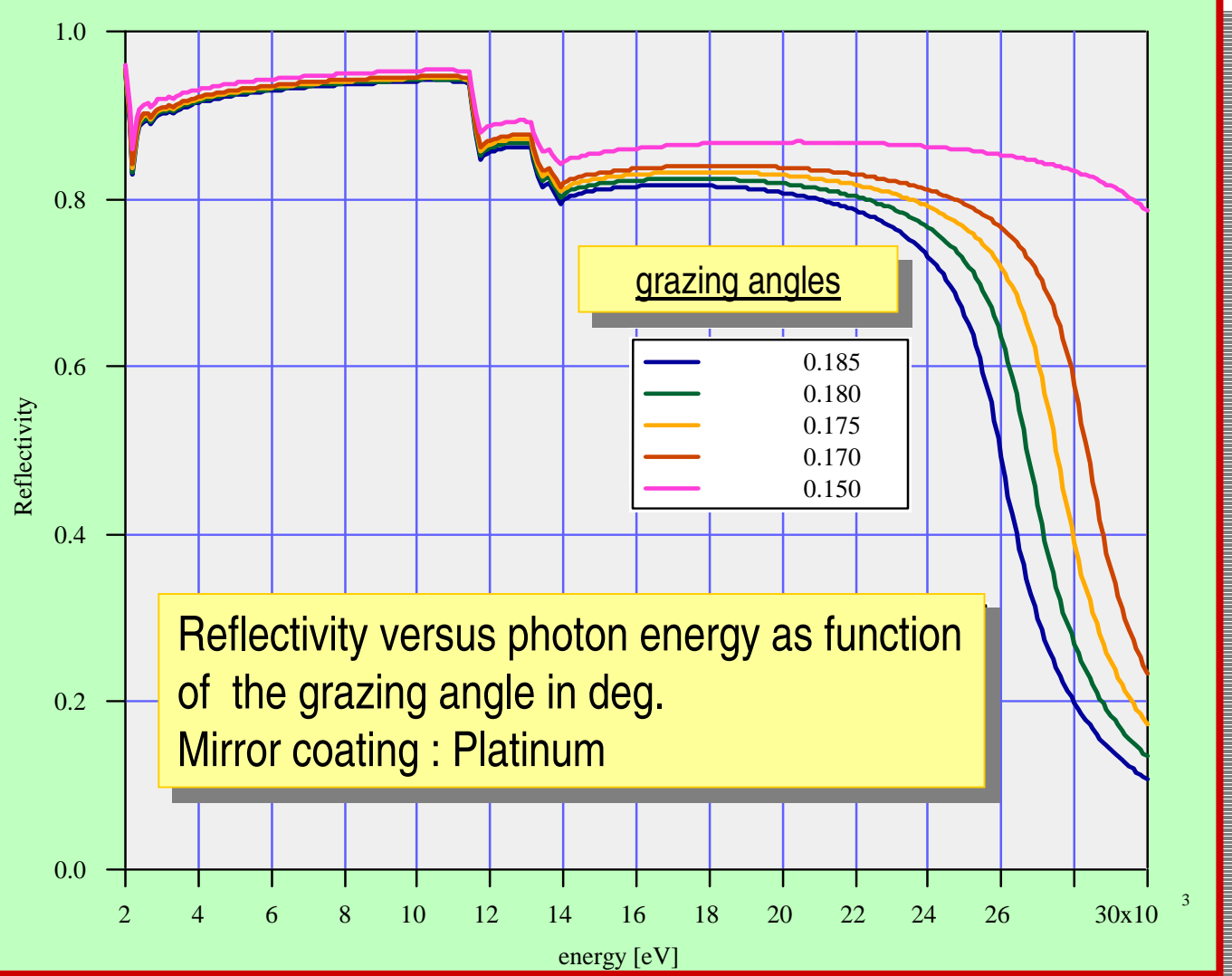


$$\vartheta = \vartheta_c$$



$$\vartheta > \vartheta_c$$

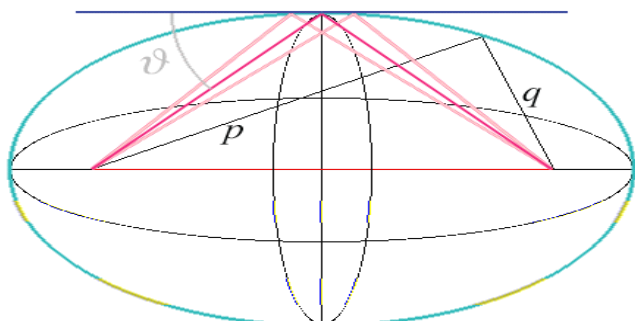




Mirrors 2: focussing

In the ideal mirror device all rays from one particular **point** are reflected and focused into another **point** according to $1/q + 1/p = 1/f$

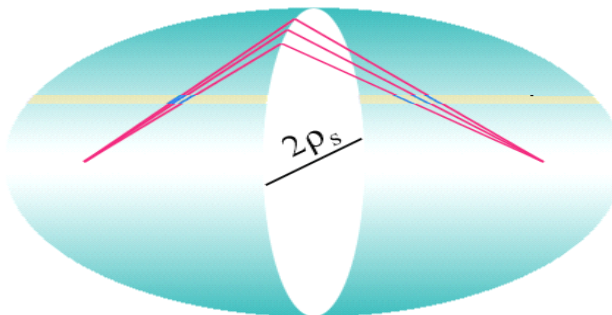
ELLIPSOIDAL SURFACE



best approximation circle

$$\rho_{tangential} = 2f / \sin \vartheta$$

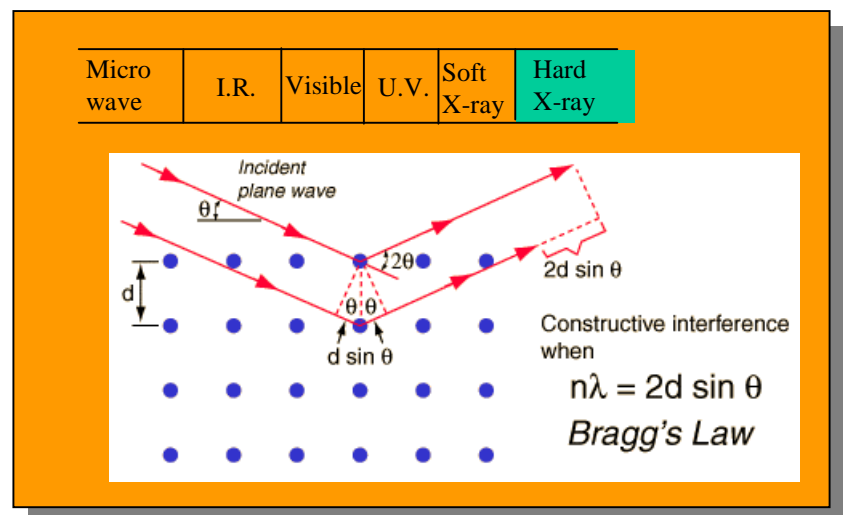
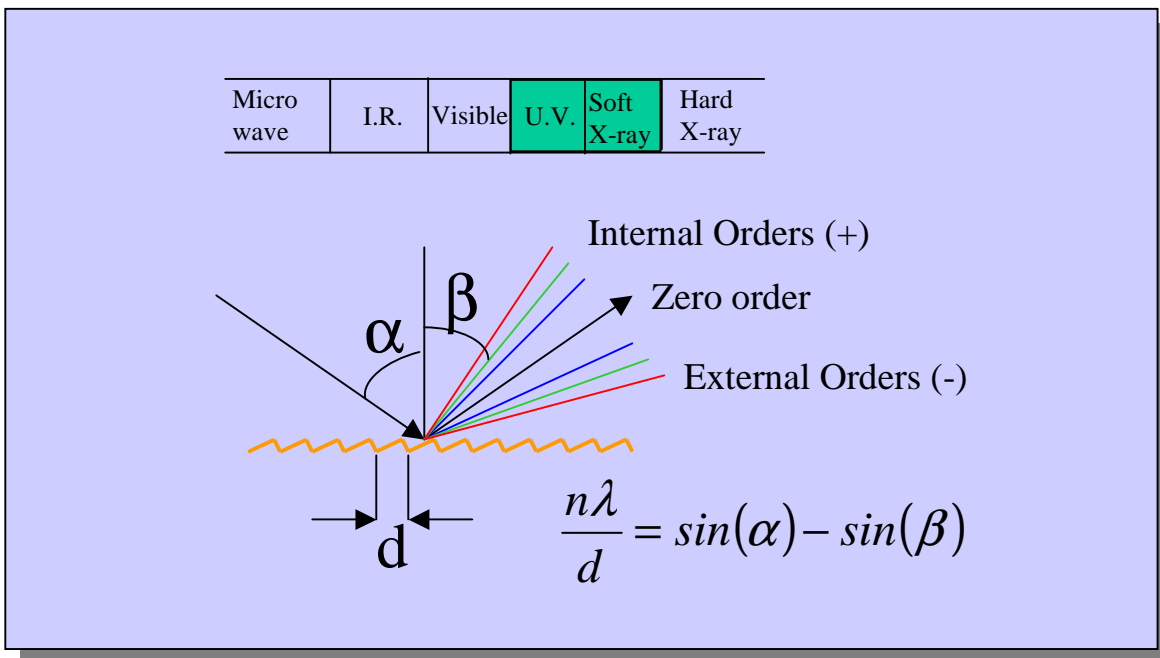
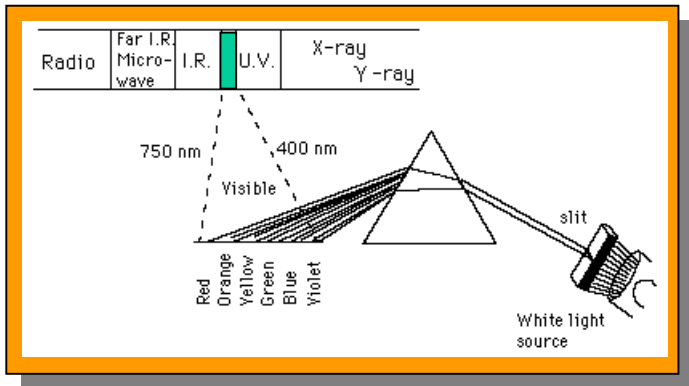
Tangential focussing

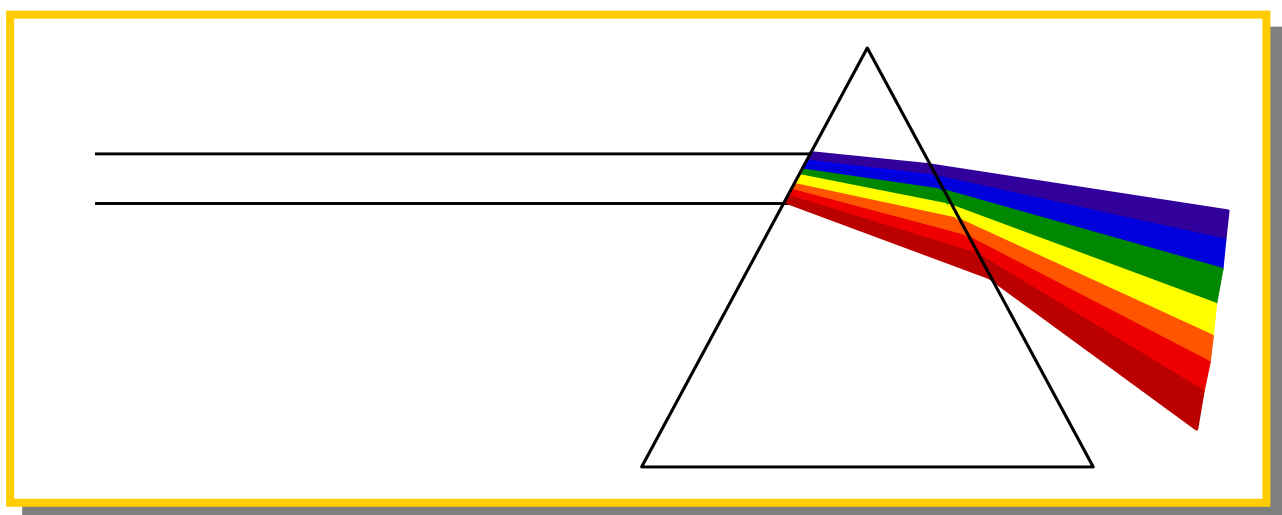


$$\rho_{sagittal} = 2f \sin \vartheta$$

Sagittal focussing

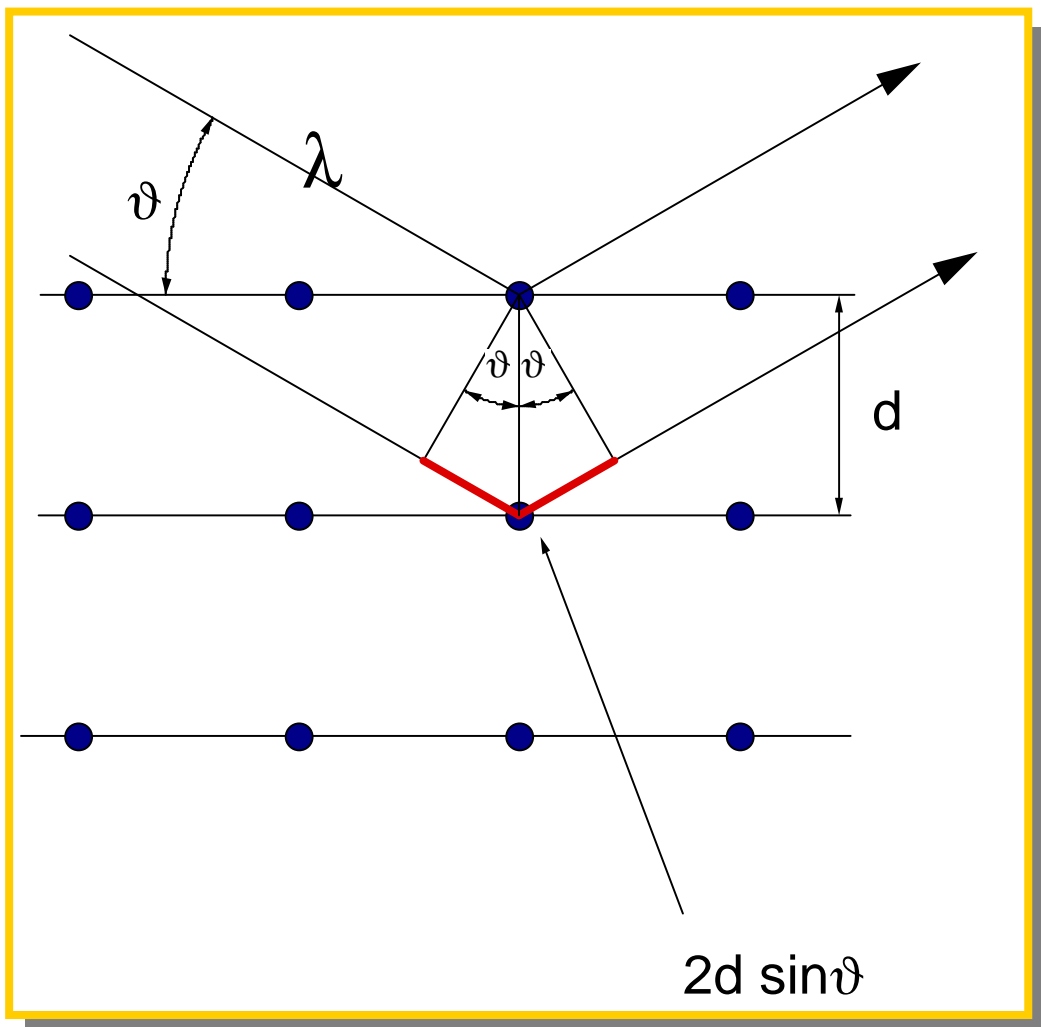
* the bending magnet case
* the extended source case





the optical prism is used to separate the components of the white visible light

sampling the out coming light with a slit it is possible to select a part of the spectrum with a spectral purity which depends on the distance and the slits aperture.



the Bragg's law

Radiation of wavelength λ is reflected by the lattice plane.

The outgoing waves interfere. The interference is constructive only if the difference of optical path is a multiple of λ :

$$2d \sin \vartheta = n\lambda$$

$$2d\sin\vartheta = n\lambda$$

from the Bragg law

$$\sin\vartheta = 1 \Rightarrow \lambda_{\max}$$

therefore

$$\lambda_{\max} = 2d$$

and the Bragg angle is 90°

important properties for the x-ray monochromators

- ENERGY RESOLUTION

$$\frac{\Delta\lambda}{\lambda} = \frac{\Delta E}{E} = \Delta\vartheta \cot g(\vartheta_B)$$

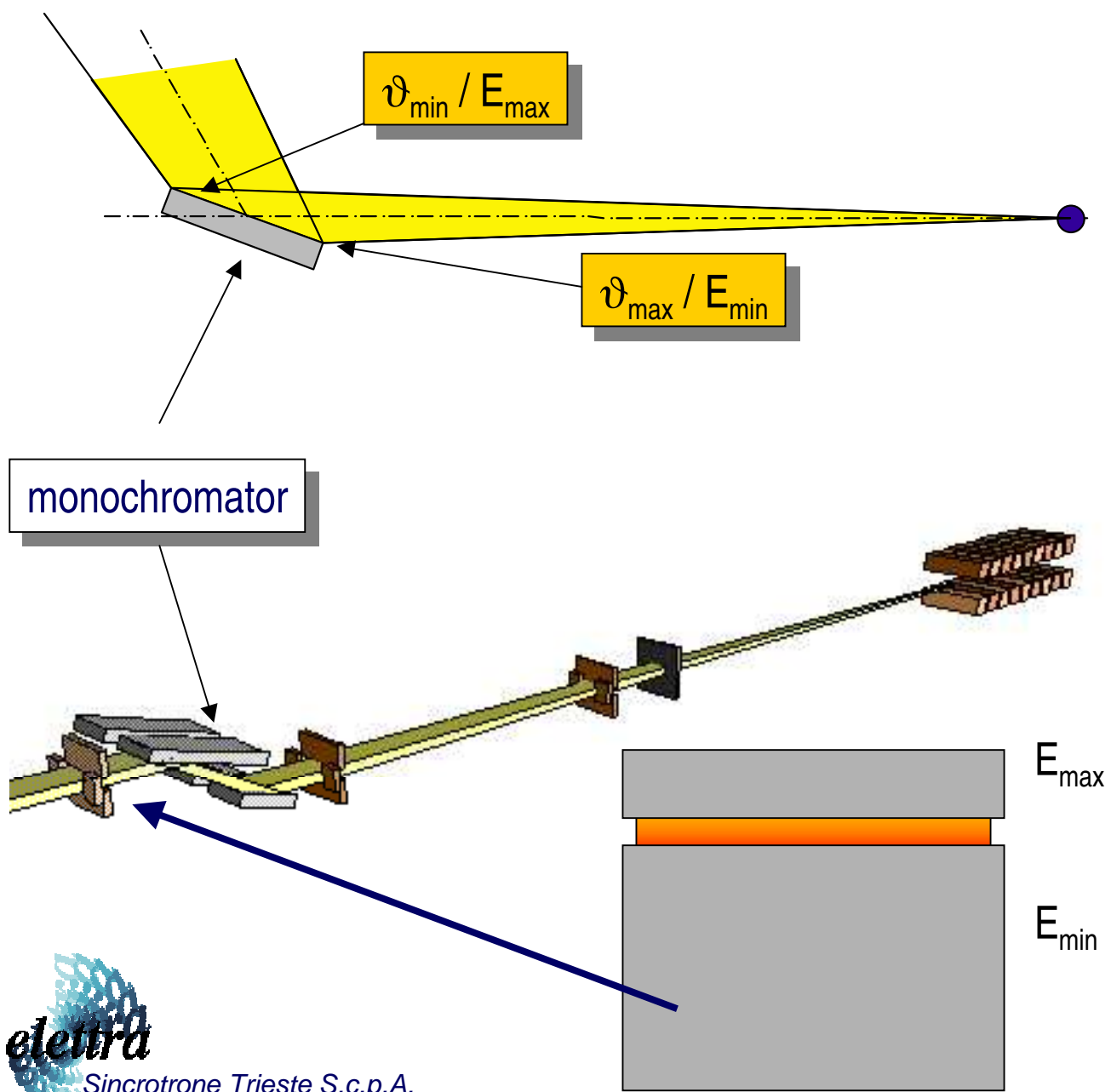
$\Delta\vartheta$ has two contribution :

- $\Delta\vartheta_{\text{beam}}$ - beam angular spread (optics)
- ω_{crystal} - intrinsic reflection width of the monochromator

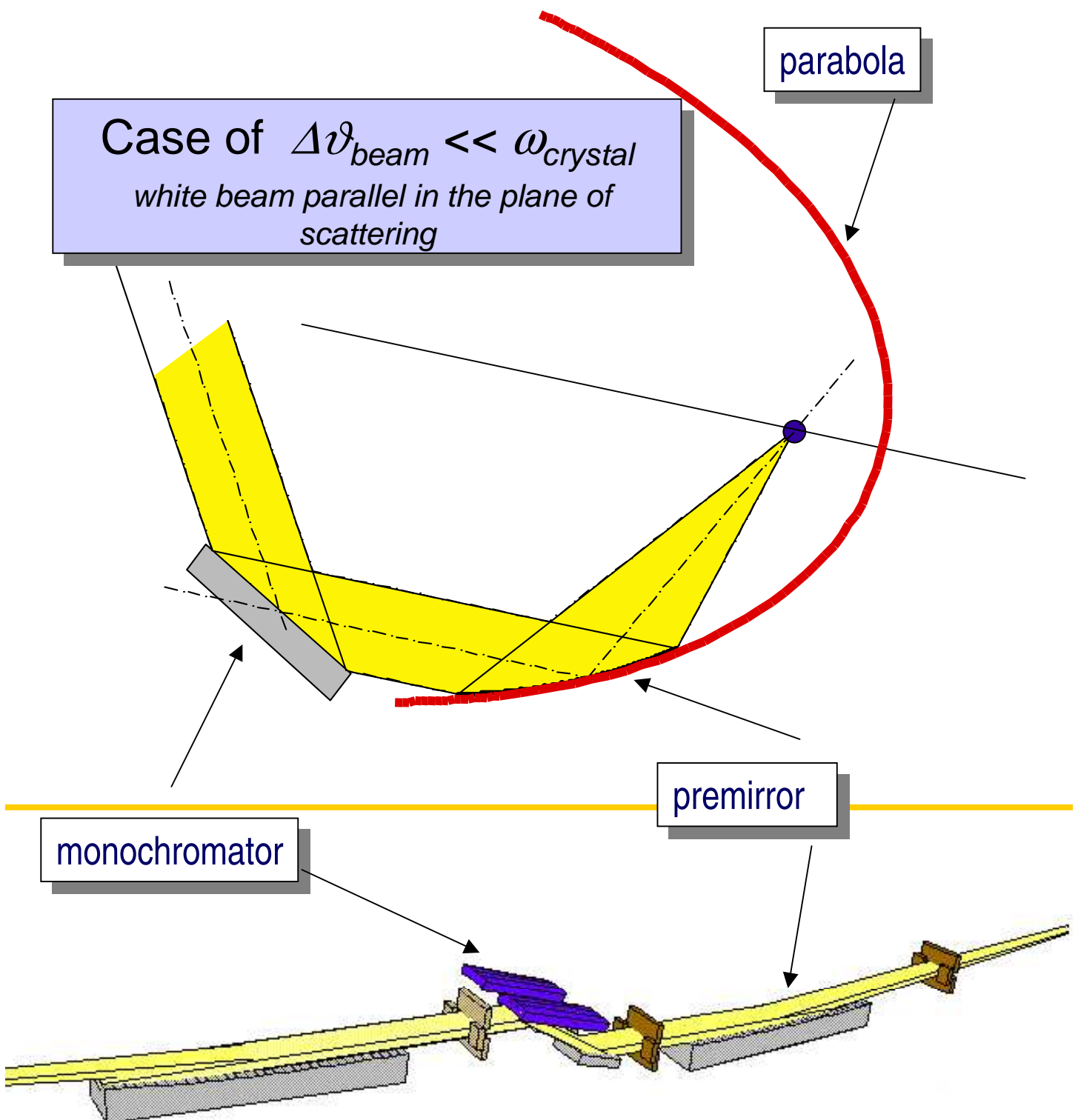
Case of $\Delta\vartheta_{beam} \gg \omega_{crystal}$

white beam with divergence in the plane of scattering

The crystal accepts all the rays with
 $\vartheta_{min} \leq \vartheta_B \leq \vartheta_{max}$



Case of $\Delta\vartheta_{beam} \ll \omega_{crystal}$
white beam parallel in the plane of scattering

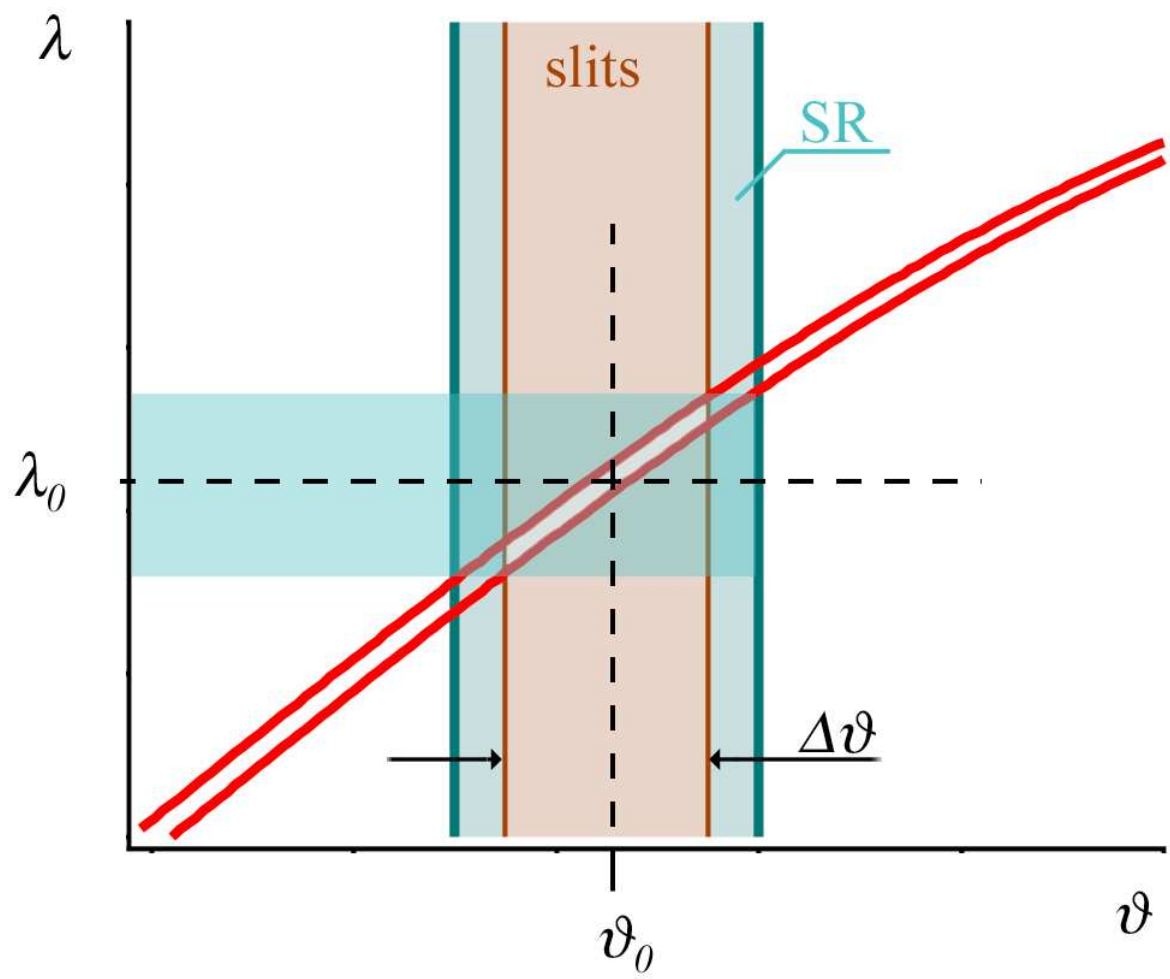


The energy bandwidth is determined by the derivative of the Bragg's law

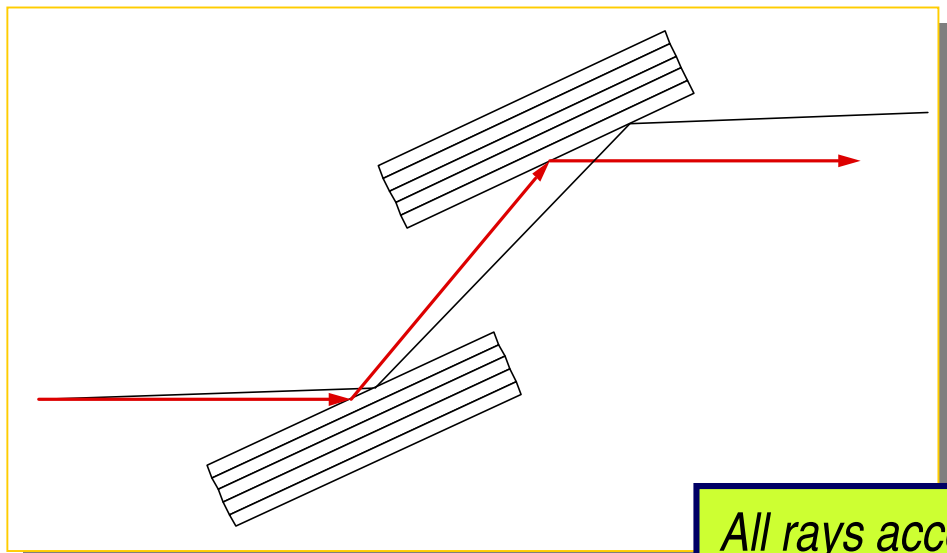
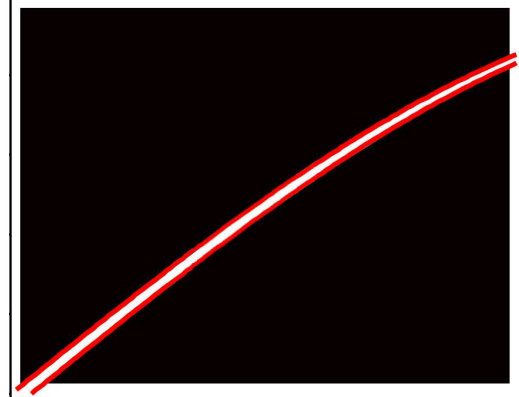
$$\Delta E = \omega_{crystal} \cotg(\vartheta_B) E$$



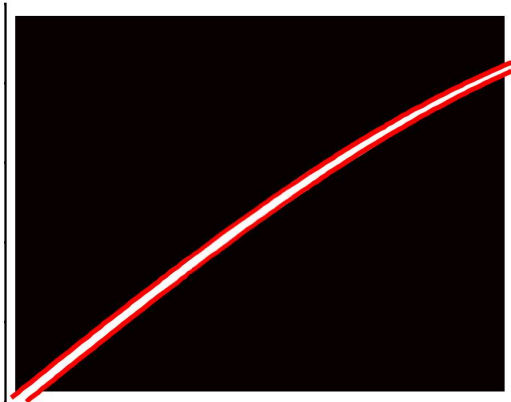
Dumond diagrams



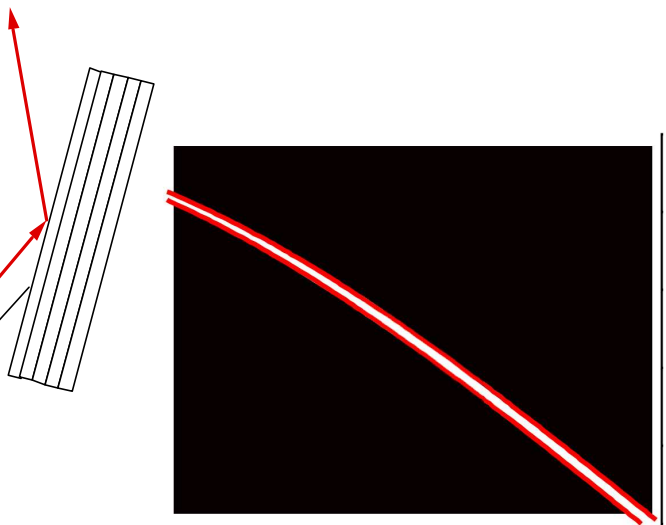
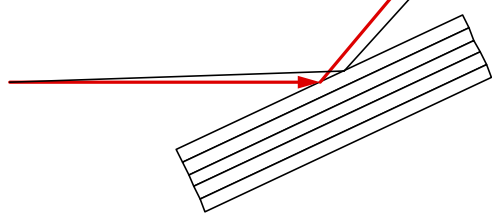
Second crystal in **non dispersive** configuration



*All rays accepted
by the first crystal
are accepted also
at the second.*

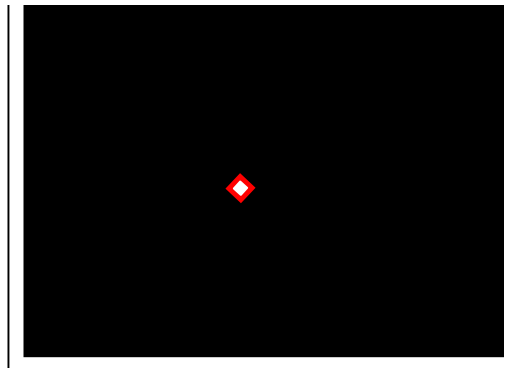
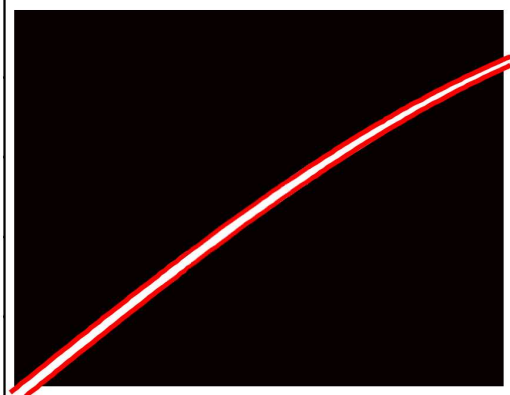


Second crystal in
dispersive configuration



Rays incident at a lower angle than the central ray on the first crystal are incident at a higher angle on the second crystal.

energy resolution ↑
intensity of the reflection ↓



*Sincrotrone Trieste S.c.p.A.
Hard-X Ray Optics
Laboratory*

two models for the x-ray diffraction in single crystals

kinematical model

apply this model for:

- thin perfect crystals
- distorted or mosaic crystals

according with Darwin model (1922) the mosaic crystal is defined by two general conditions:

- crystallites have to be **misoriented** more than the Darwin width of the perfect crystal (loss of the phase condition)
- their dimensions have to be smaller than the **extinction length** of the considered radiation (no second interaction)

dynamical model

apply this model for:

- thick and perfect crystal

a) we can't longer consider single interaction.
(extinction length)

b) we can't neglect, as well as in the kinematical model, the effect of the radiation absorption

INTENSITY OF THE REFLECTION

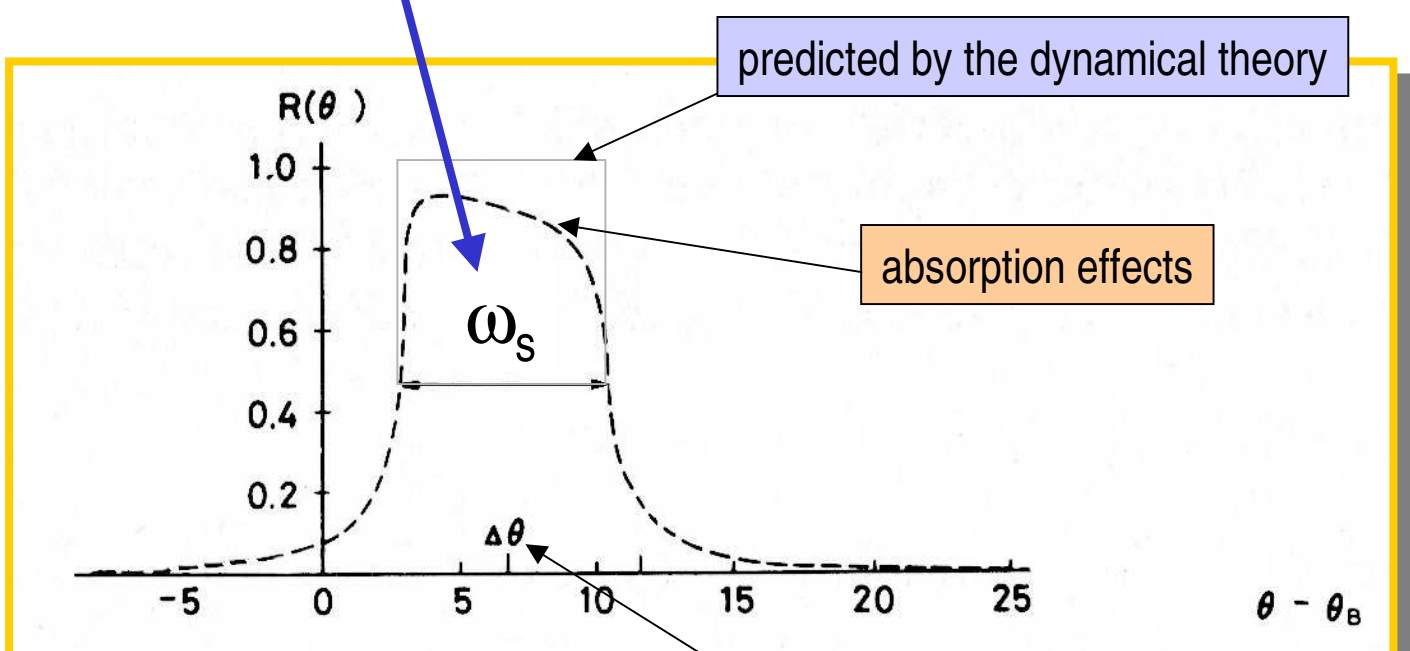
- reflectivity or peak reflectivity
- integral reflecting power

The Darwin curve

$$\omega_s = \frac{2}{\sin 2\vartheta_B} \frac{r_e \lambda^2}{\pi V} C F_{hr} |e^{-M}|$$

n order of the reflection
 λ_1 wavelength of the fundamental
 $e^{M(n)}$ temperature factor
 V volume of the unit cell
 ϑ_B Bragg angle
 R_e radius of the electron e^2/mc^2

F_{hr} real part of the structure factor related to the diffracted direction $\mathbf{h}(h,k,l)$



angular shift due to the refractive effect



the **b** parameter defined as :

$$b = \frac{\sin(\alpha - \vartheta_B)}{\sin(\alpha + \vartheta_B)}$$

α is the angle between the Bragg plane and the crystal surface

T. Matsushita and H. Hashizume *X-Ray Monochromators*
Handbook on Synchrotron Radiation, Vol. 1

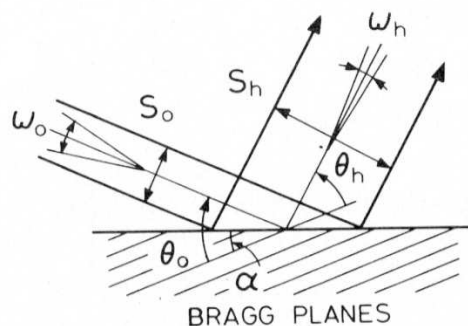


Fig. 3. Geometry of X-ray reflection by a perfect single crystal. θ_0 : incidence angle; θ_h : reflection angle. For a non-zero asymmetry angle α ($0 < |\alpha| < \theta_B$), the angular width ω_0 for acceptance is not equal to the angular width ω_h for emergence. The figure is drawn for $b < 1.0$, where $\omega_0 > \omega_s > \omega_h$. Note also the change of beam cross sections, S_0 and S_h .

$$\omega_0 = \frac{\omega_s}{\sqrt{b}}$$

the angular acceptance as function of the intrinsic width and the **b** parameter:

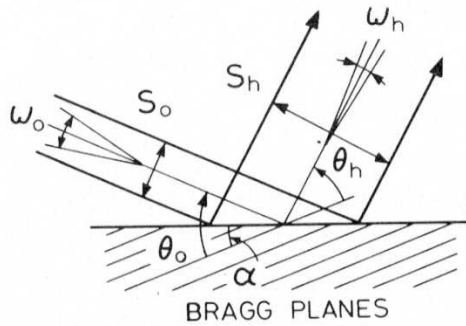


Fig. 3. Geometry of X-ray reflection by a perfect single crystal. θ_0 : incidence angle; θ_h : reflection angle. For a non-zero asymmetry angle α ($0 < |\alpha| < \theta_B$), the angular width ω_0 for acceptance is not equal to the angular width ω_h for emergence. The figure is drawn for $b < 1.0$, where $\omega_0 > \omega_s > \omega_h$. Note also the change of beam cross sections, S_0 and S_h .

Bragg reflection width in case of asymmetric cut crystal is defined by:

$$\omega_h = \omega_s \sqrt{b}$$

$$\omega_h = b\omega_0$$

the angular acceptance as function of the Bragg reflection width

also for the beams sections

$$S_h = \frac{S_0}{b}$$

combining the two formulas we have the well known Liouville's theorem

$$\omega_h S_h = \omega_0 S_0$$

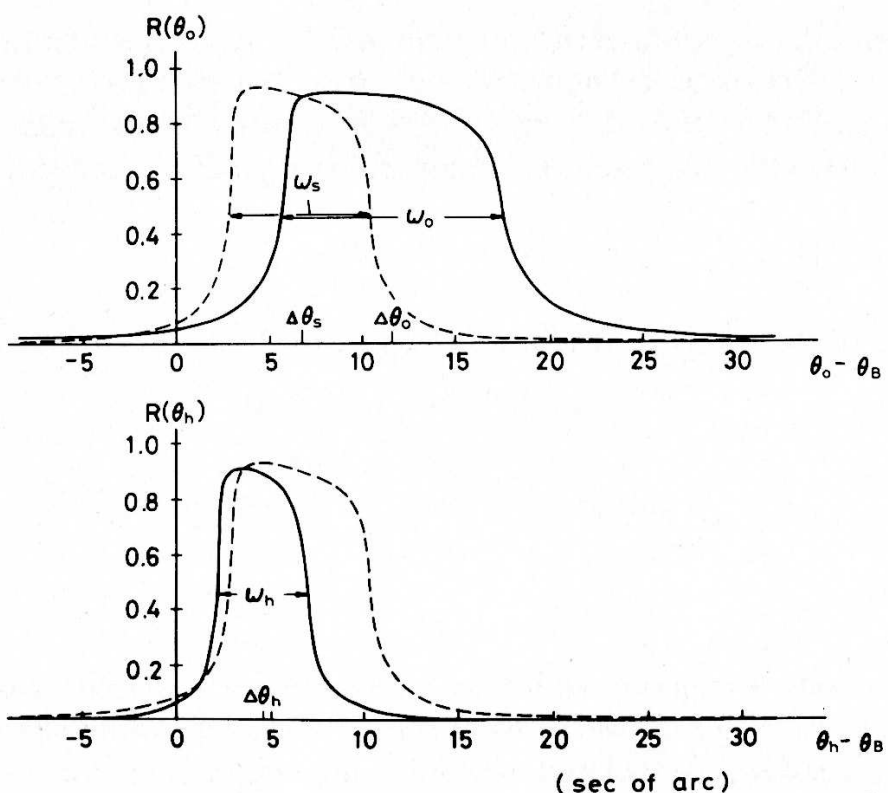
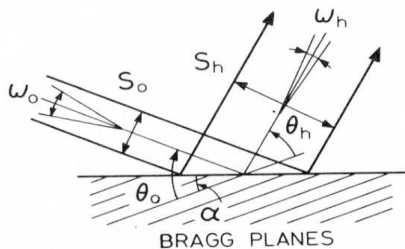


Fig. 4. Perfect-crystal reflection curves for the (111) reflection of silicon at 1.6 \AA . $R(\theta_0)$ shows the reflectivity for the ideal plane wave as a function of the incidence angle θ_0 , while $R(\theta_h)$ represents the intensity reflected at a reflection angle θ_h for a plane wave incident at θ_0 , θ_0 and θ_h being related by $(\theta_h - \theta_B) = b(\theta_0 - \theta_B)$. The solid curves are calculated for an asymmetric case of $b = 0.4$, while the broken curves for the symmetric case ($b = 1.0$) where $R(\theta_0) \equiv R(\theta_h)$.

T. Matsushita and H. Hashizume **X-Ray Monochromators**
Handbook on Synchrotron Radiation, Vol. 1, edited by E.E. Kock
North-Holland Publishing Company, 1983

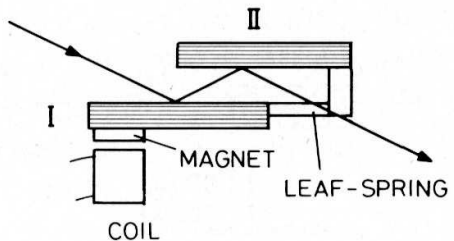
Table 2
**Intrinsic Bragg reflection widths ω_s , energy resolutions $\Delta E/E$ and
integral reflecting powers I of perfect crystals of silicon, germanium
and α -quartz at 1.54 Å.**

Crystal	<i>hkl</i>	ω_s (second or arc)	$\Delta E/E$ ($\times 10^5$)	I ($\times 10^6$)
Silicon	111	7.395	14.1	39.9
	220	5.459	6.04	29.7
	311	3.192	2.90	16.5
	400	3.603	2.53	19.3
	331	2.336	1.44	11.8
	422	2.925	1.47	15.5
	333		0.88	9.9
	(511)	1.989		
	440	2.675	0.96	14.0
	531	1.907	0.60	9.3
Germanium	111	16.338	32.64	85.9
	220	12.449	14.46	67.4
	311	7.230	6.92	37.1
	400	7.951	5.94	42.3
	331	5.076	3.34	25.4
	422	6.178	3.34	32.4
	333		2.00	20.2
	(511)	4.127		
	440	5.339	2.14	27.5
	531	3.719	1.33	17.7
α -quartz	100	3.798	10.00	18.8
	101	7.453	15.26	40.9
	110	2.512	3.69	12.2
	102	2.488	3.36	12.9
	200	2.252	2.81	11.5
	112	2.927	3.03	15.5
	202	2.072	1.93	10.6
	212	2.042	1.47	10.7
	203	2.430	1.74	12.9
	301	2.368	1.69	12.6

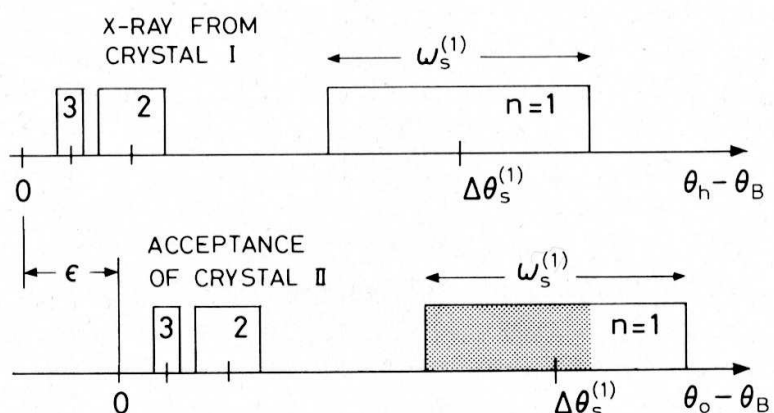
*T. Matsushita and H. Hashizume X-Ray Monochromators
Handbook on Synchrotron Radiation, Vol. I*



Sincrotrone Trieste S.c.p.A.
Hard-X Ray Optics
Laboratory



(a)



(b)

Fig. 33. An off-set harmonics-rejection monochromator. (a) Geometry of the monochromator. (b) The principle of harmonics rejection. Perfect-crystal reflection curves for the fundamental ($n = 1$) and the harmonics ($n = 2, 3$) are approximated by rectangular boxes. ϵ : off-set or misalignment angle. The shaded area represents delivered X-rays (Hart and Rodrigues 1978).

*T. Matsushita and H. Hashizume X-Ray Monochromators
Handbook on Synchrotron Radiation, Vol. 1*

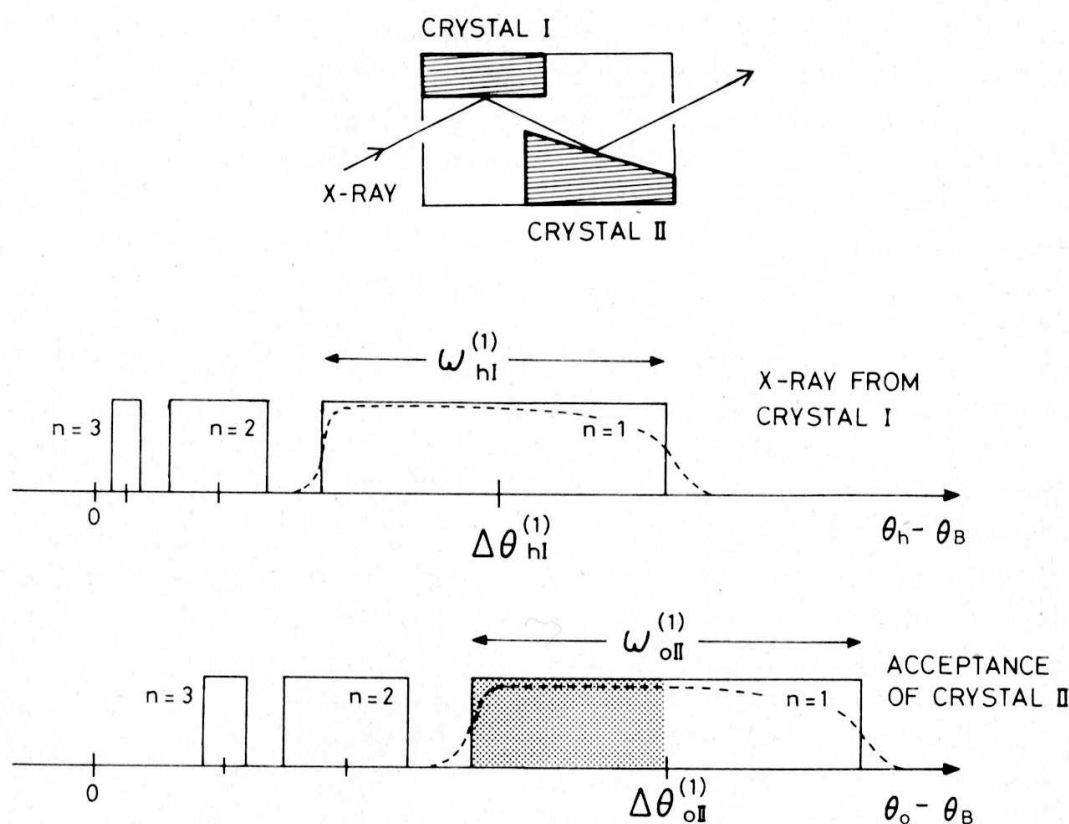
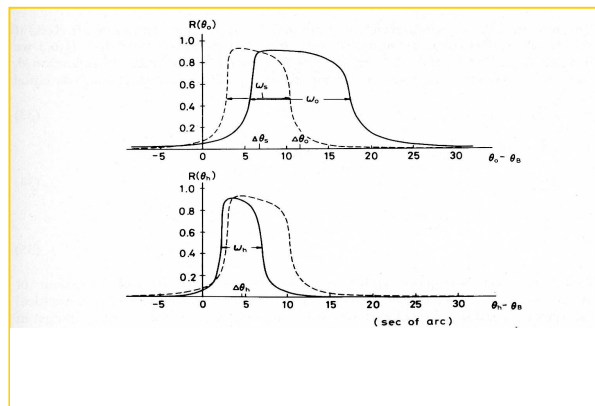
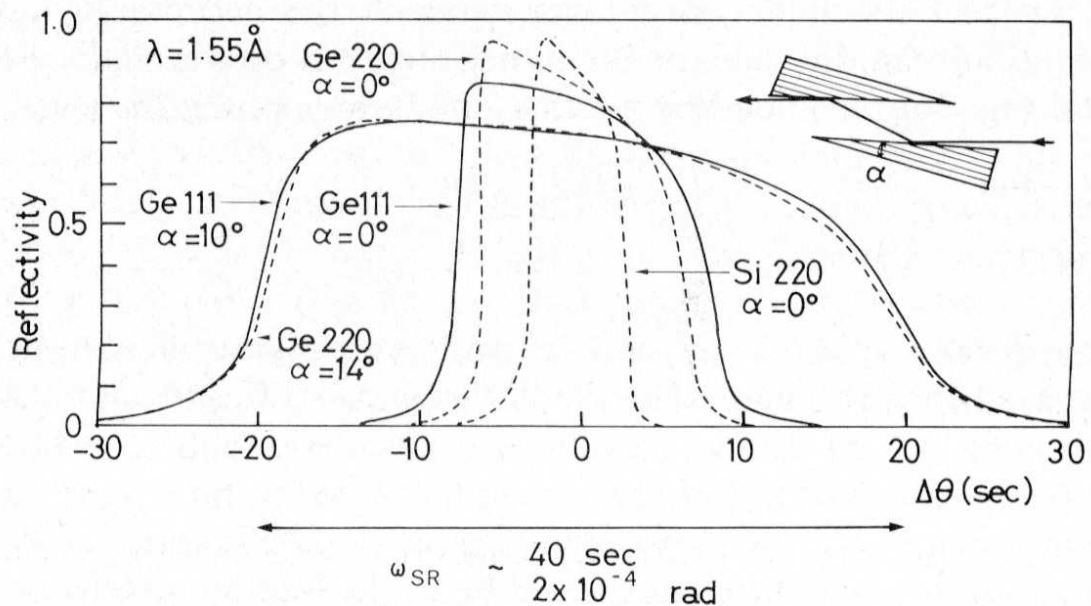


Fig. 34. A monolithic harmonics-rejection monochromator. (a) Crystals I and II of unequal asymmetry factors are built as two outstanding parts of a perfect single crystal. (b) The principle of harmonics rejection. Perfect-crystal reflection curves for the fundamental ($n = 1$) and the harmonics ($n = 2, 3$) are approximated by rectangular boxes. The broken curves show the real reflection curves for the fundamental. The shaded area represents delivered X-rays.

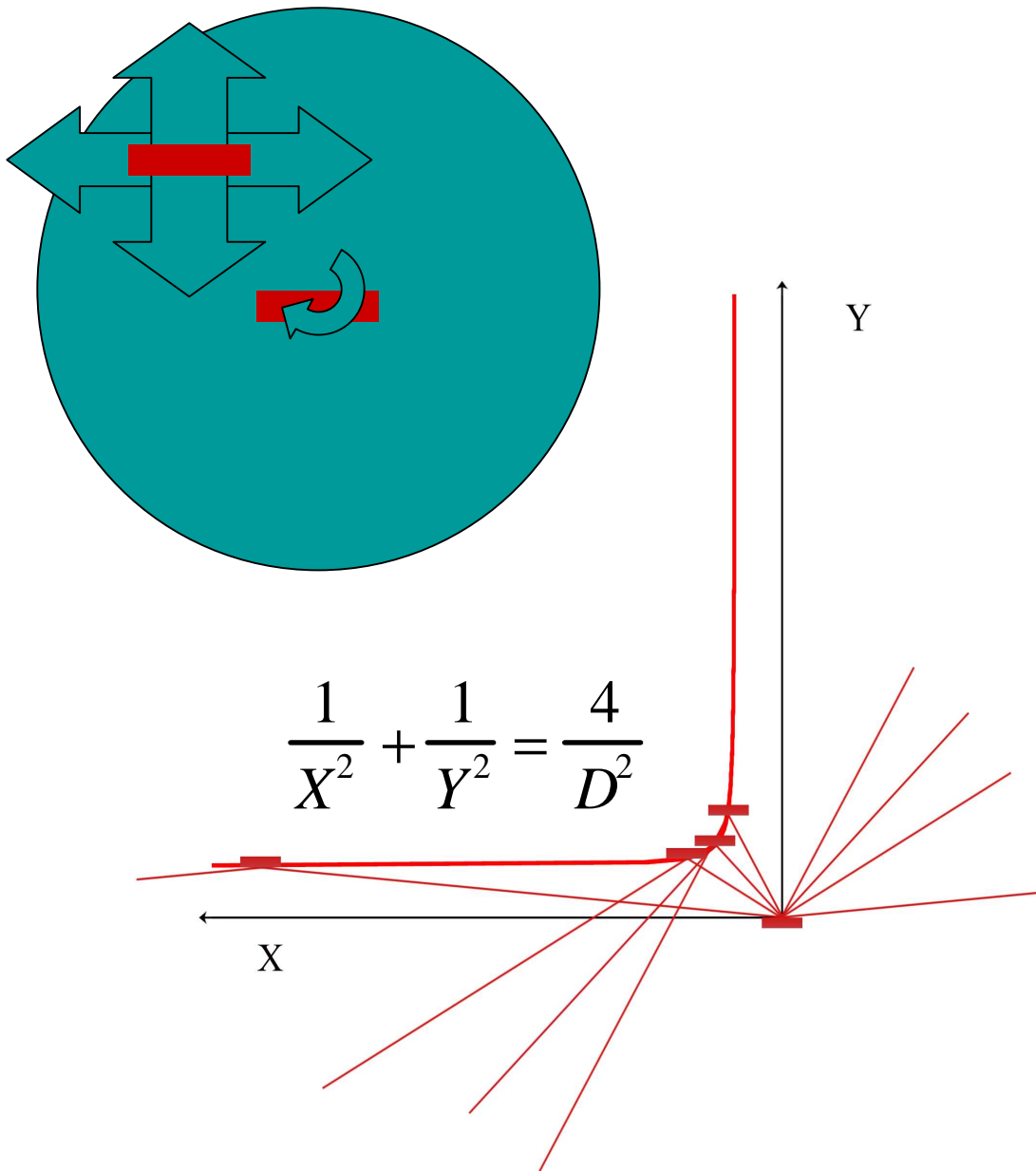


Calculated reflectivity curves of grooved monochromators using various asymmetric reflections of silicon and germanium for 1.55 \AA X-rays (Kohra et al. 1978).

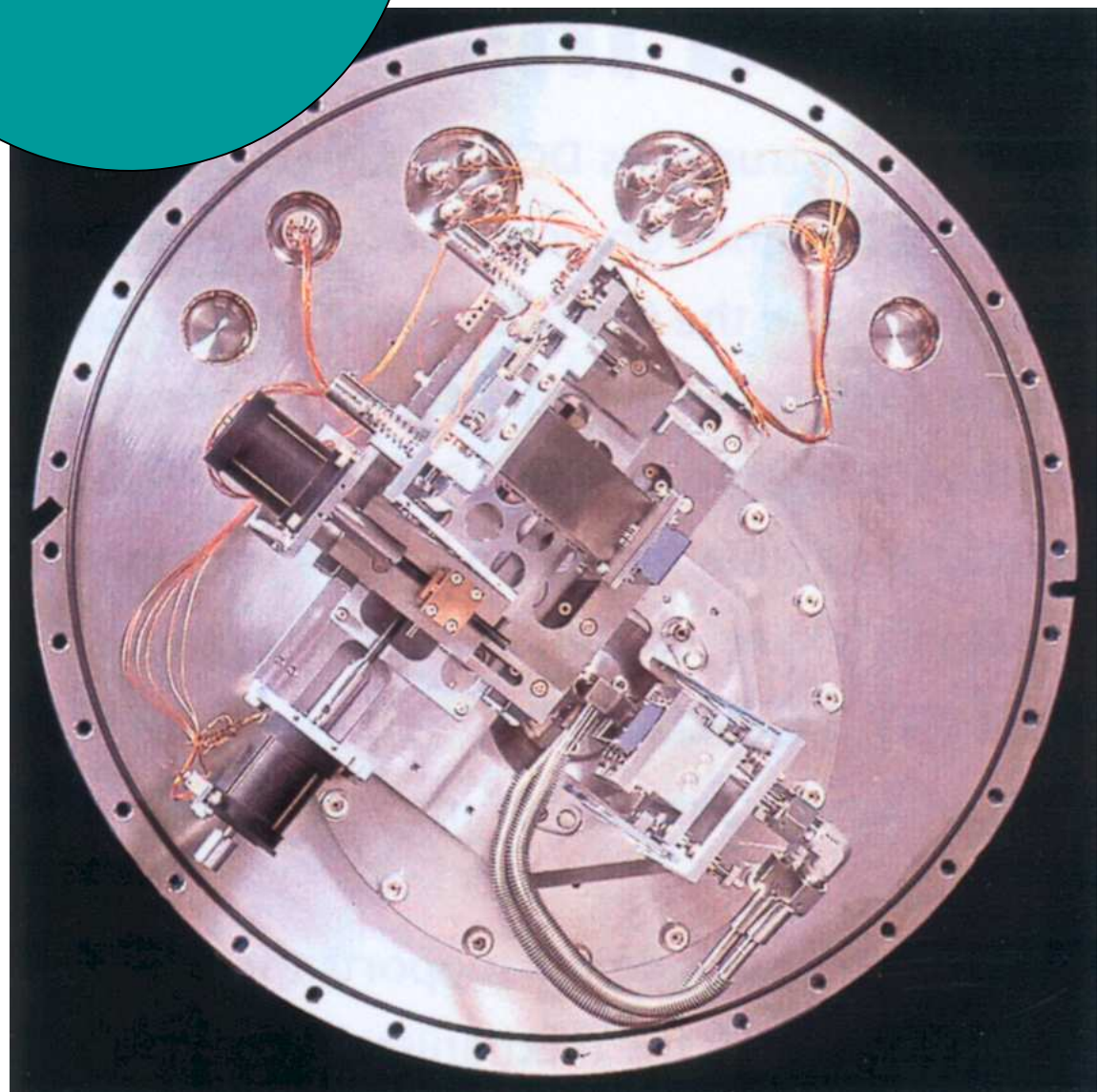
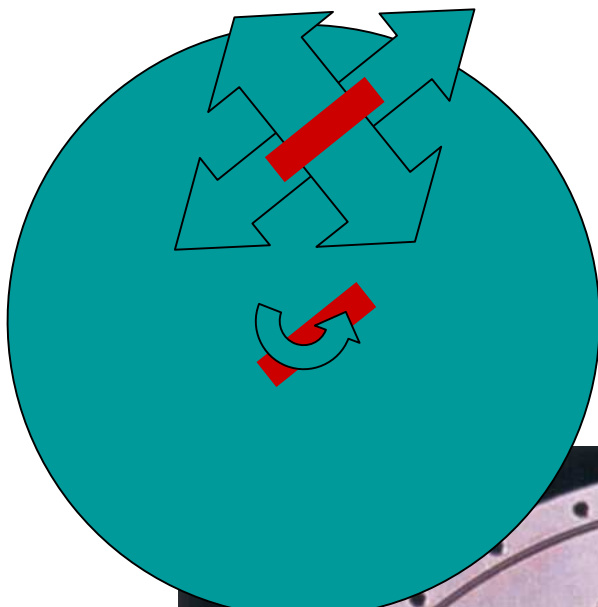
*T. Matsushita and H. Hashizume X-Ray Monochromators
Handbook on Synchrotron Radiation, Vol. 1*

Note as the refractive effect on the first crystal
has been totally compensated by the second one

Double crystal monochromator

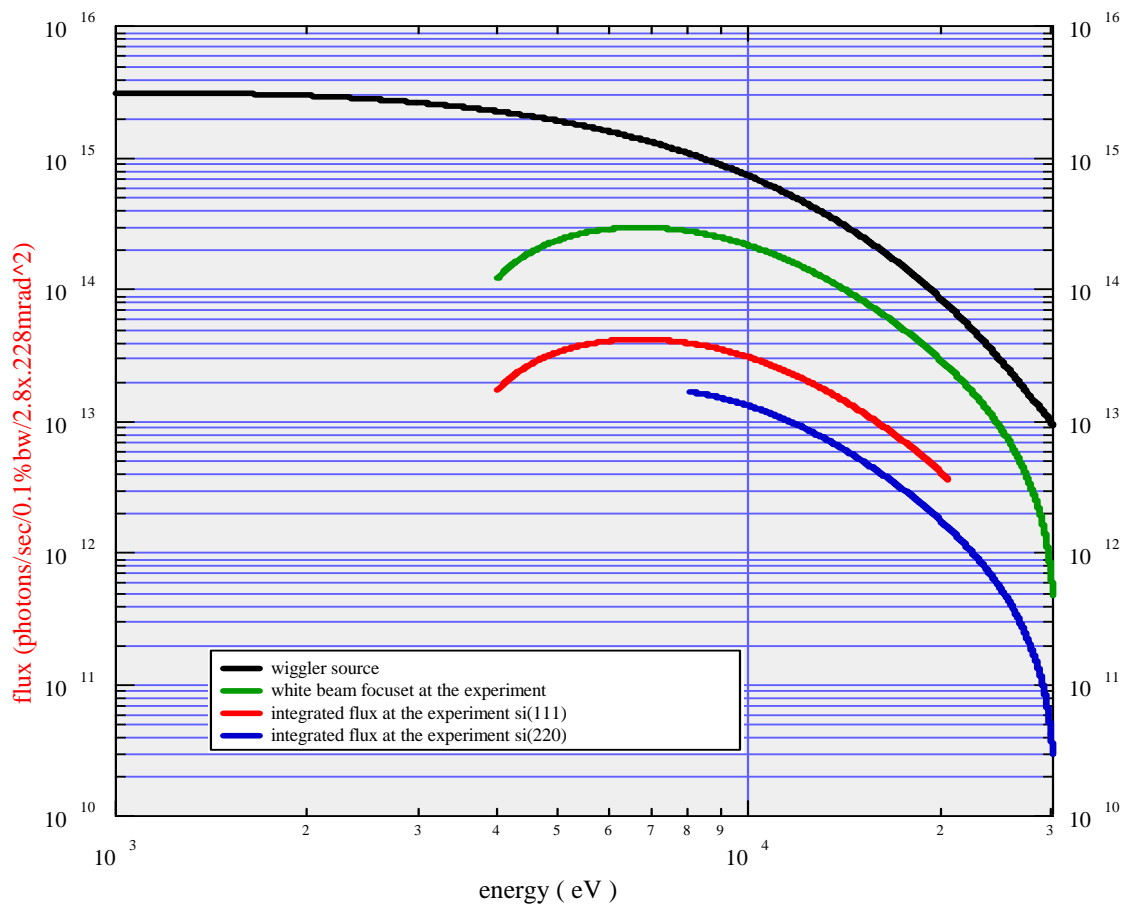


Double crystal monochromator



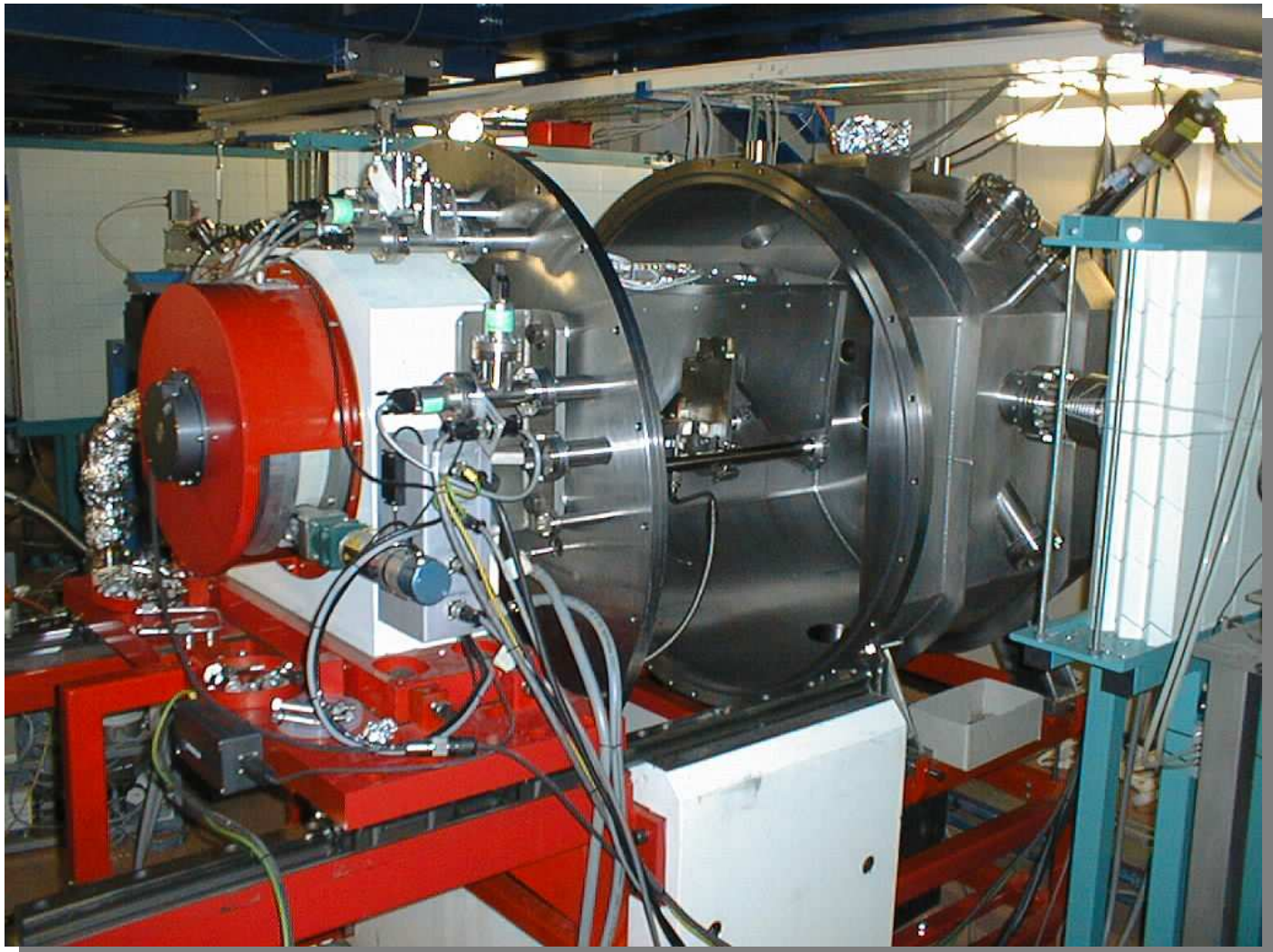
Diffraction 1

57 poles wiggler source at ELETTRA
400mA, 1.6T and 2GeV
total power: 8 kW



Sincrotrone Trieste S.c.p.A.
Hard-X Ray Optics
Laboratory

The double crystal monochromator at the **diffraction1** beamline



Sincrotrone Trieste S.c.p.A.
Hard-X Ray Optics
Laboratory

Diffraction 1:

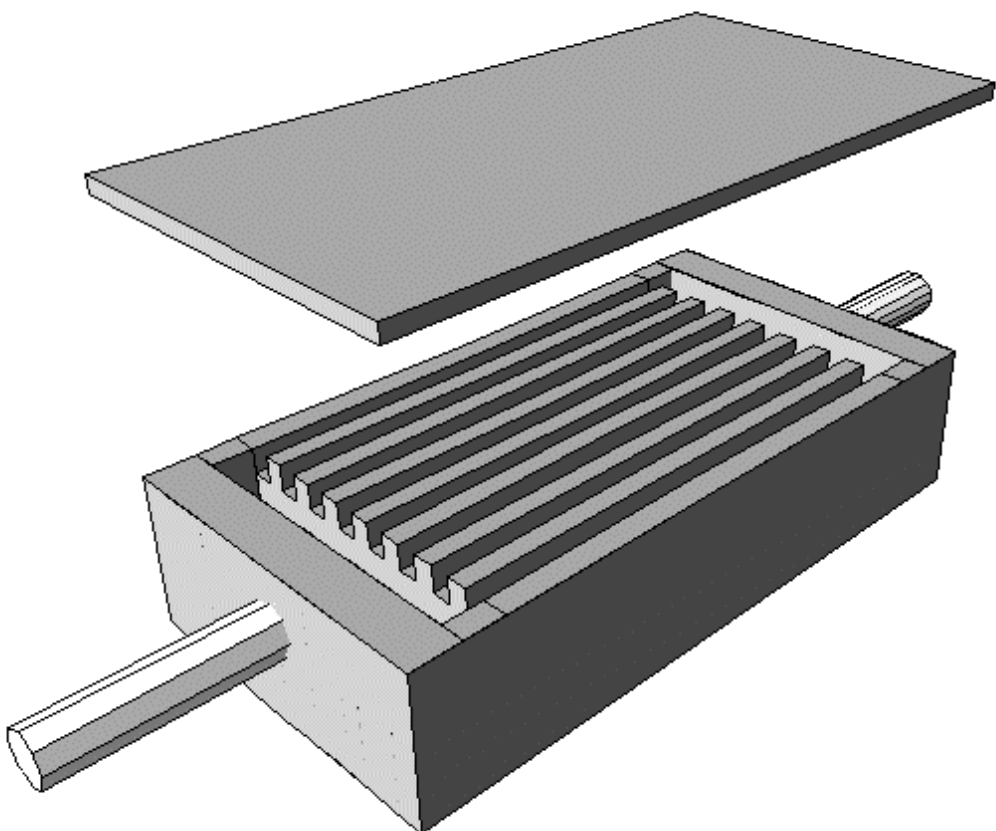
first optical element in the beam
Si(111) internally water cooled

total power absorbed 0.5 kW*

* $1.5 \times 0.28 \text{ mrad}^2$

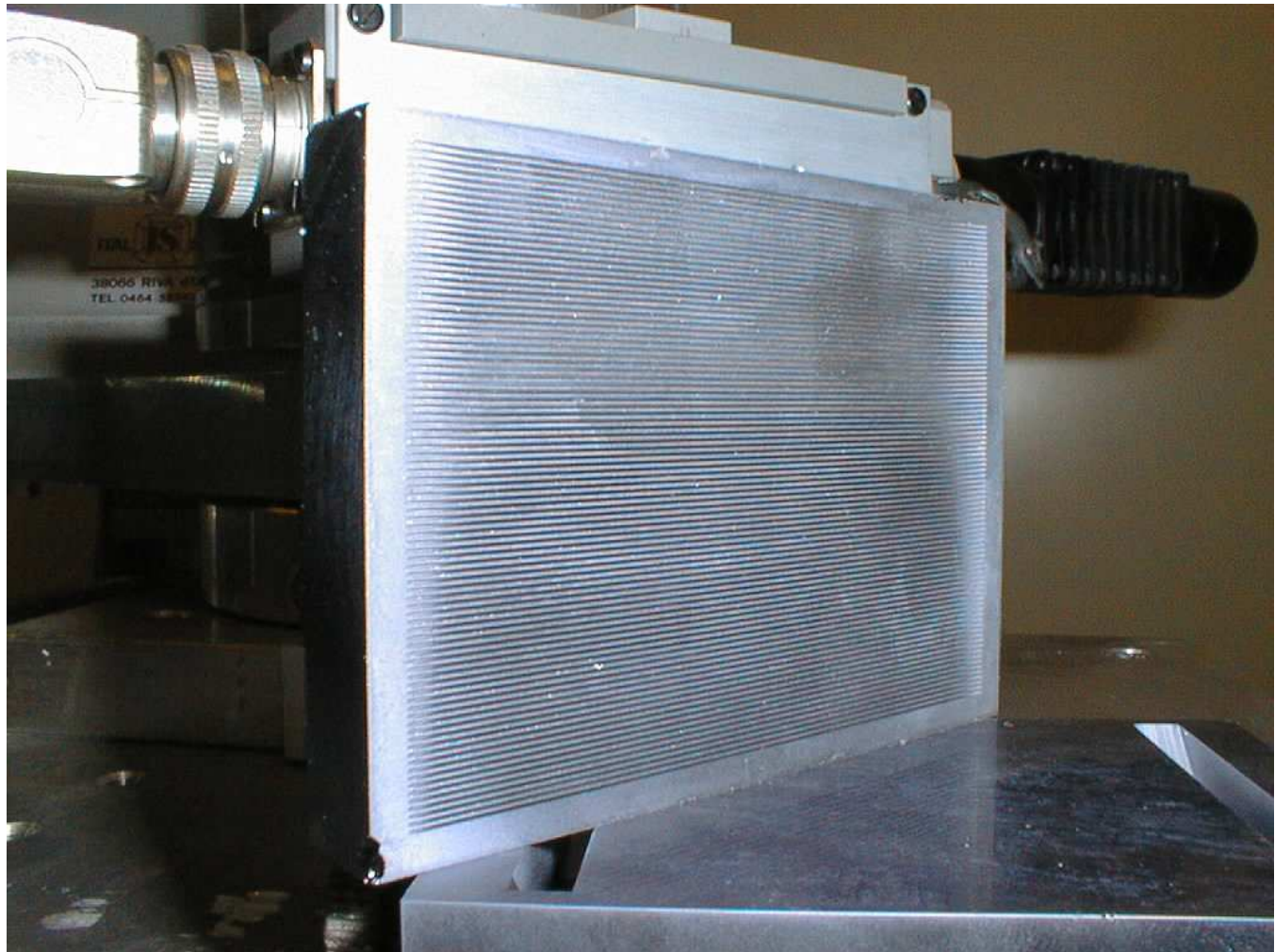


Conceptual design of an internally water cooled crystal



Sincrotrone Trieste S.c.p.A.
Hard-X Ray Optics
Laboratory

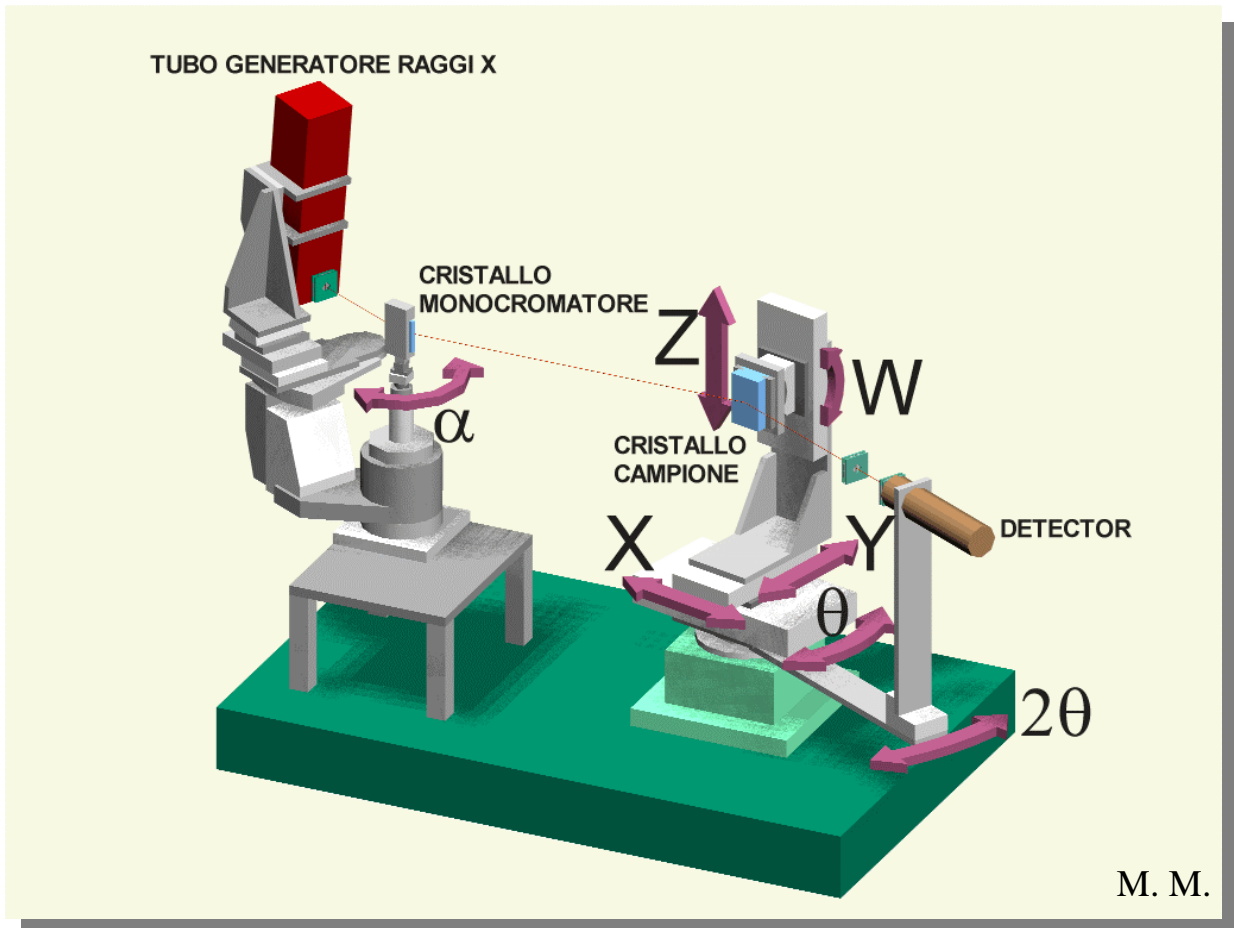
The two Si components before the Si-Si brazing



channels:

thickness: 300 μ m
depth: 2mm

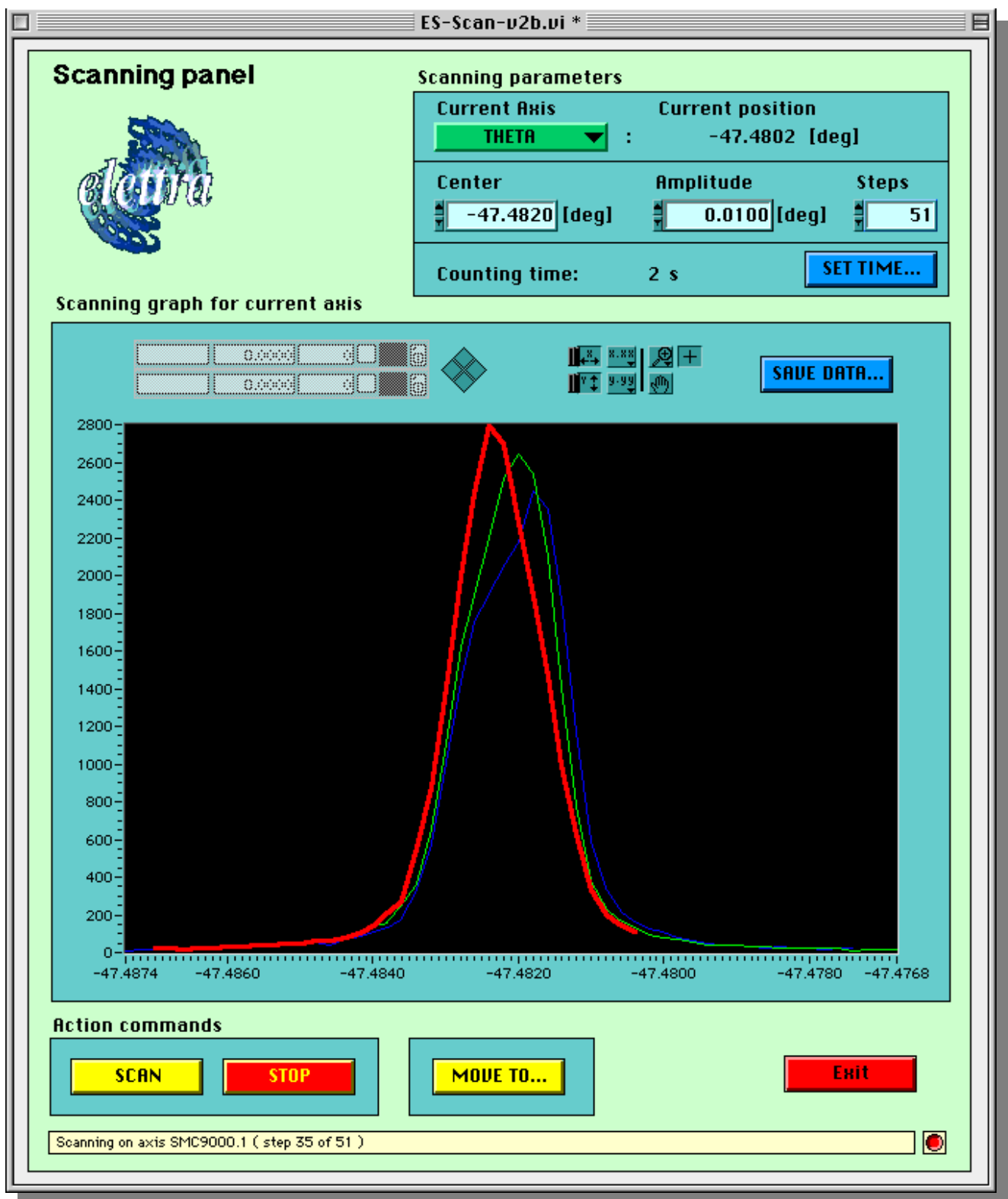
3D picture of the double ϑ - 2ϑ equipment



The double ϑ - 2ϑ test station at the Hard X-ray Laboratory

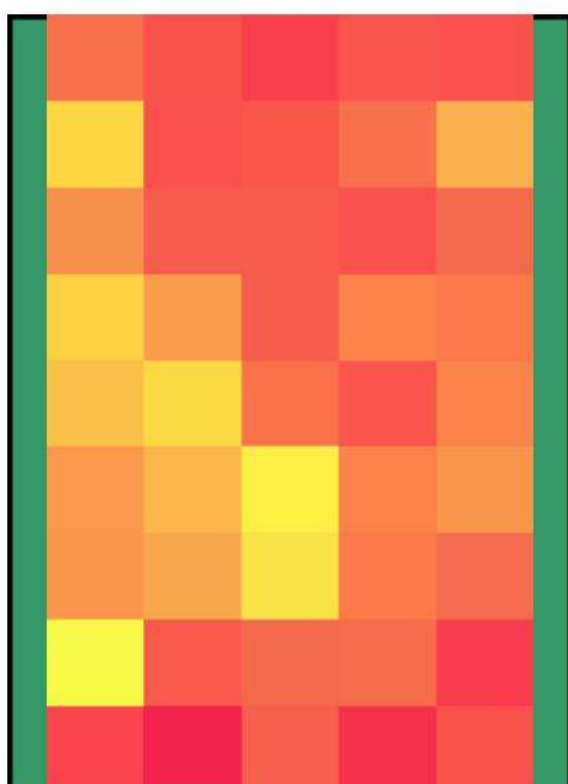


Sincrotrone Trieste S.c.p.A.
Hard-X Ray Optics
Laboratory



Sincrotrone Trieste S.c.p.A.
Hard-X Ray Optics
Laboratory

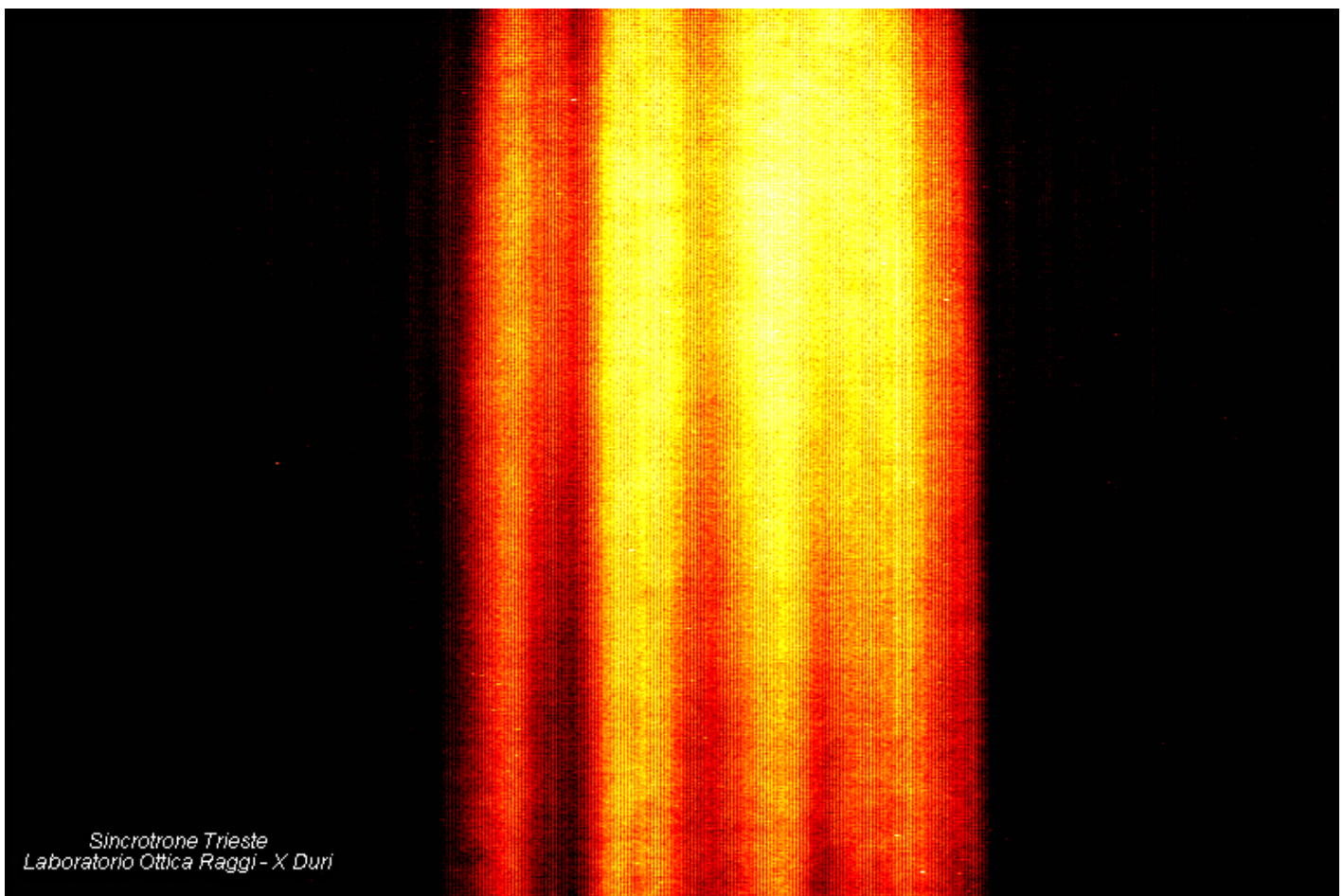
**DISTRIBUZIONE DELL'AMPIEZZA DELLE ROCKING-CURVE
VALUTATE MEDIANTE DIFFRAZIONE SUI PIANI Si-111**



14.1
13.6
13.1
12.6
12.1
11.6
11.1
10.7
10.2
9.7

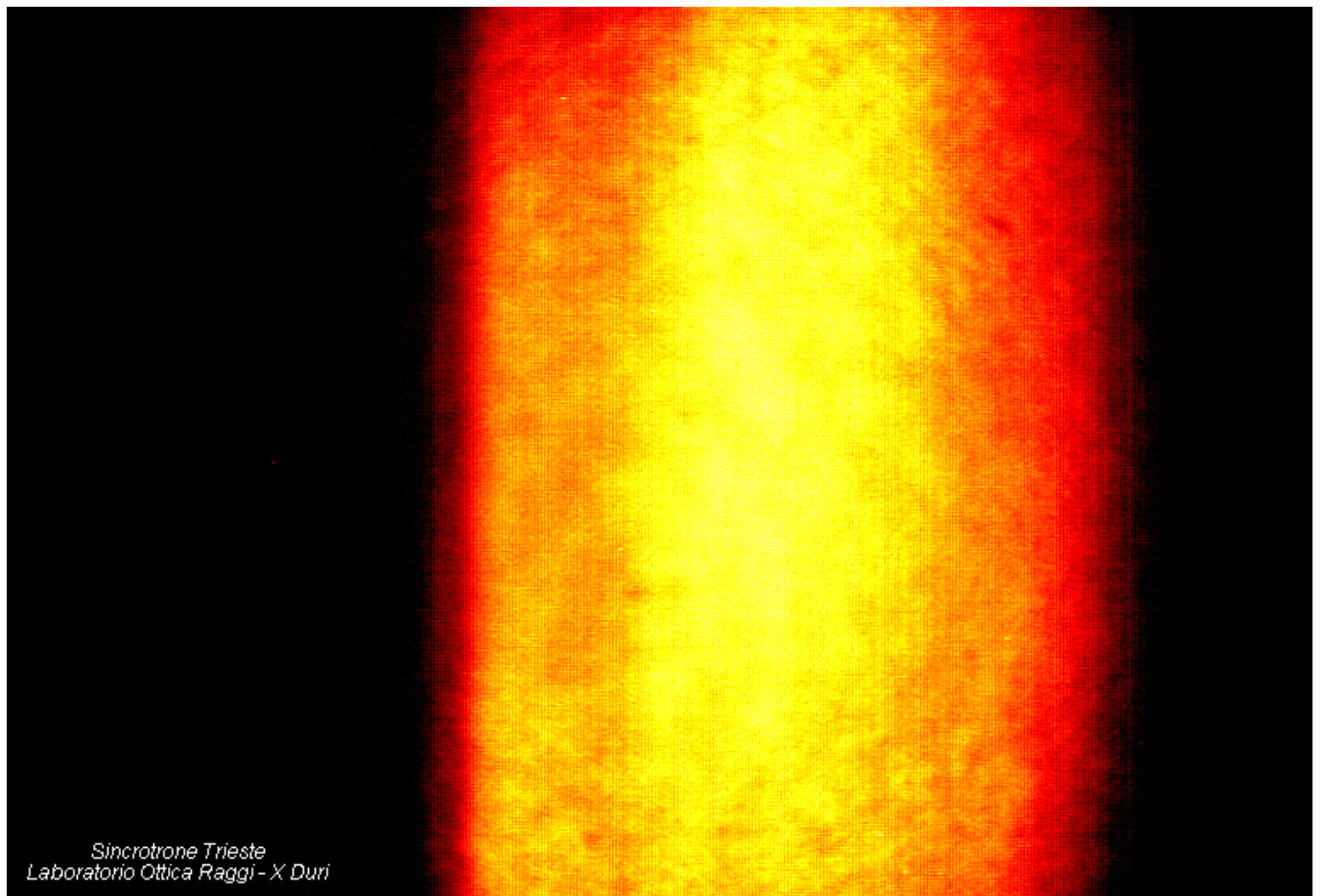
**Valori espressi in
secondi di grado**

Topography of the internal cooled Si-crystal with channels perpendicular to the scattering plane



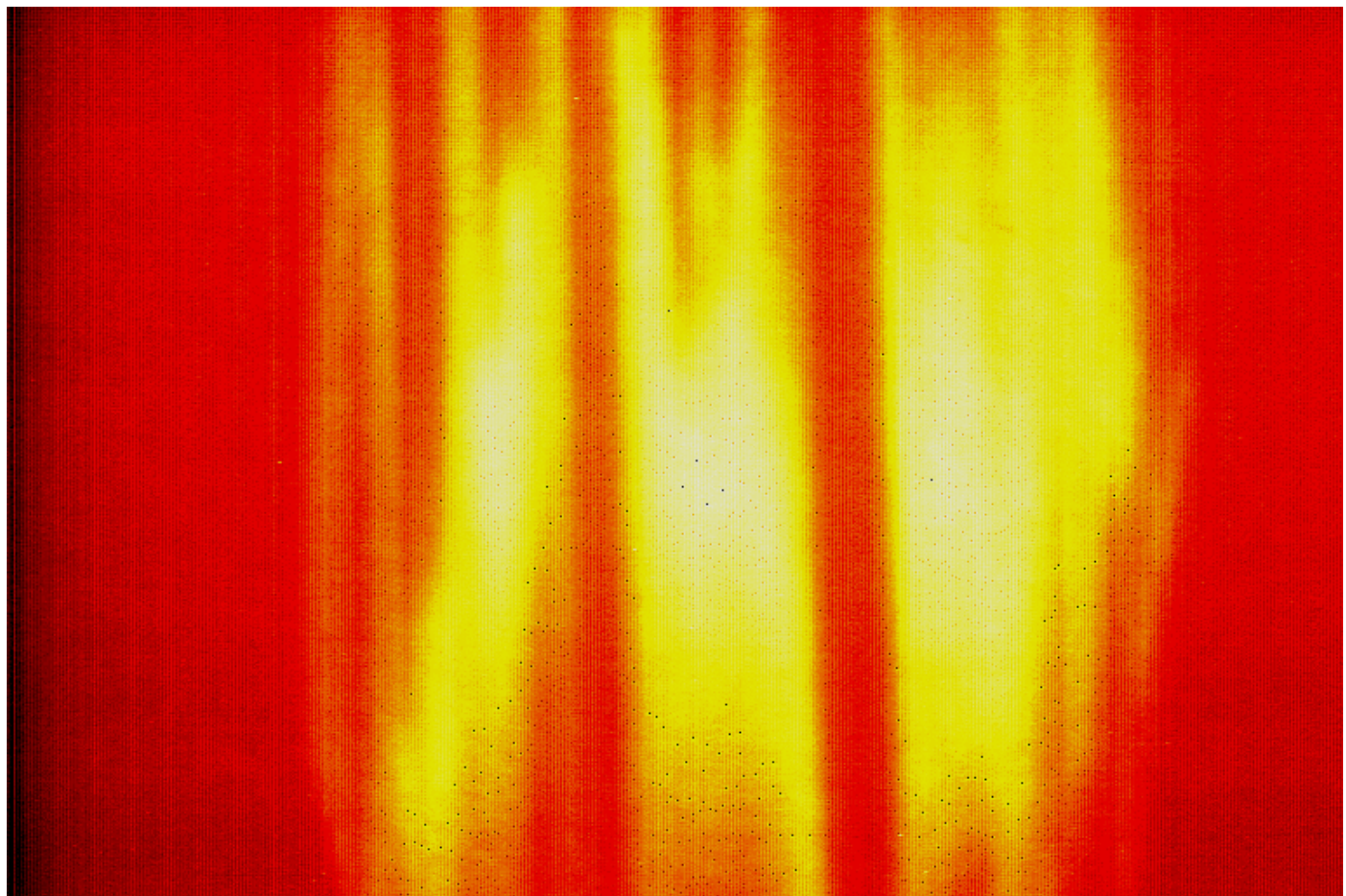
Sincrotrone Trieste S.c.p.A.
Hard-X Ray Optics
Laboratory

Same topography but with
channels in the same direction of
the scattering plane



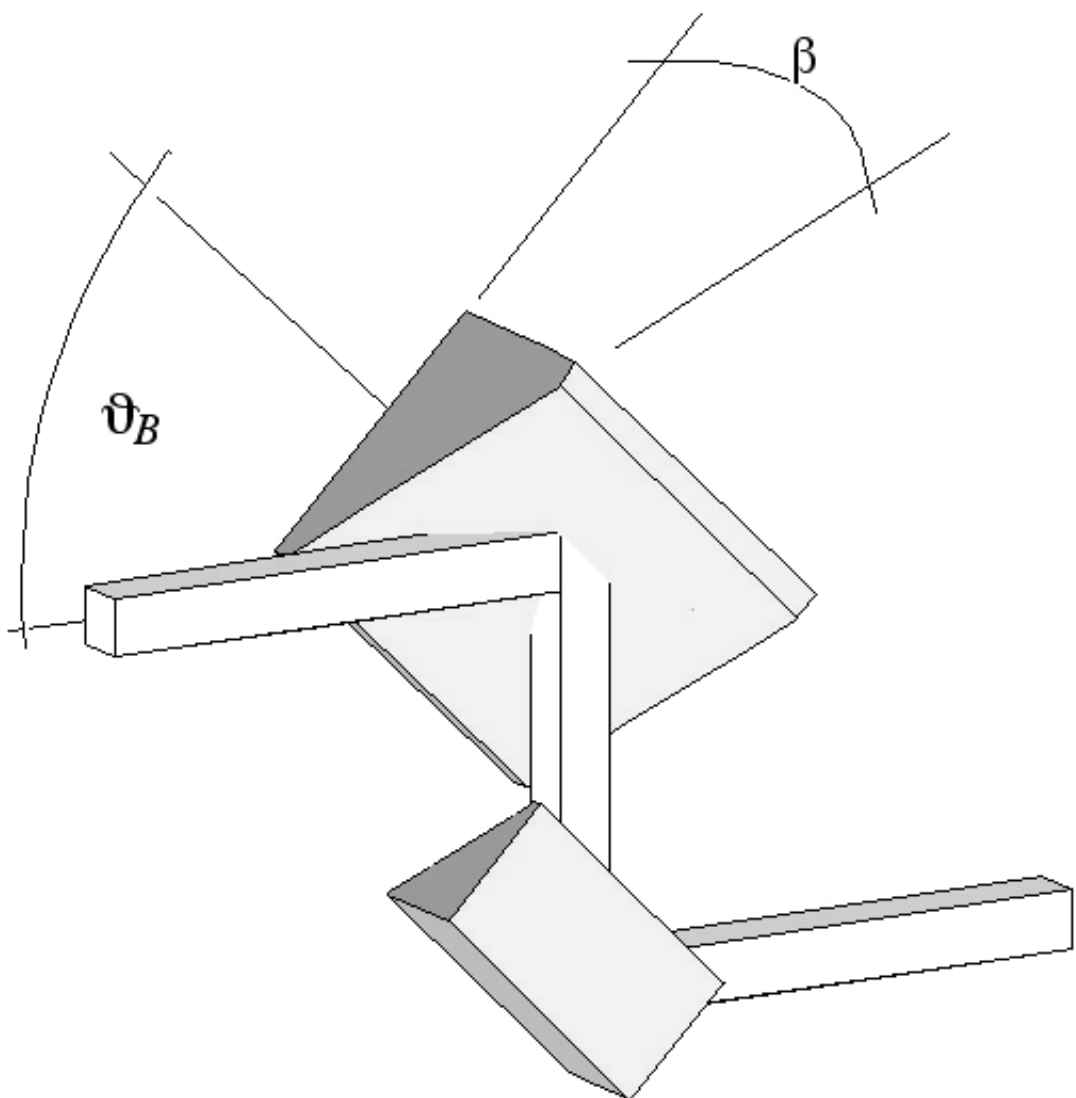
Sincrotrone Trieste S.c.p.A.
Hard-X Ray Optics
Laboratory

surface of a Si(111) crystal with a evident stressed structure induced by a back-side machining and not removed by chemical hatching



Sincrotrone Trieste S.c.p.A.
Hard-X Ray Optics
Laboratory

The inclined double crystal monochromator setup to reduce the power density

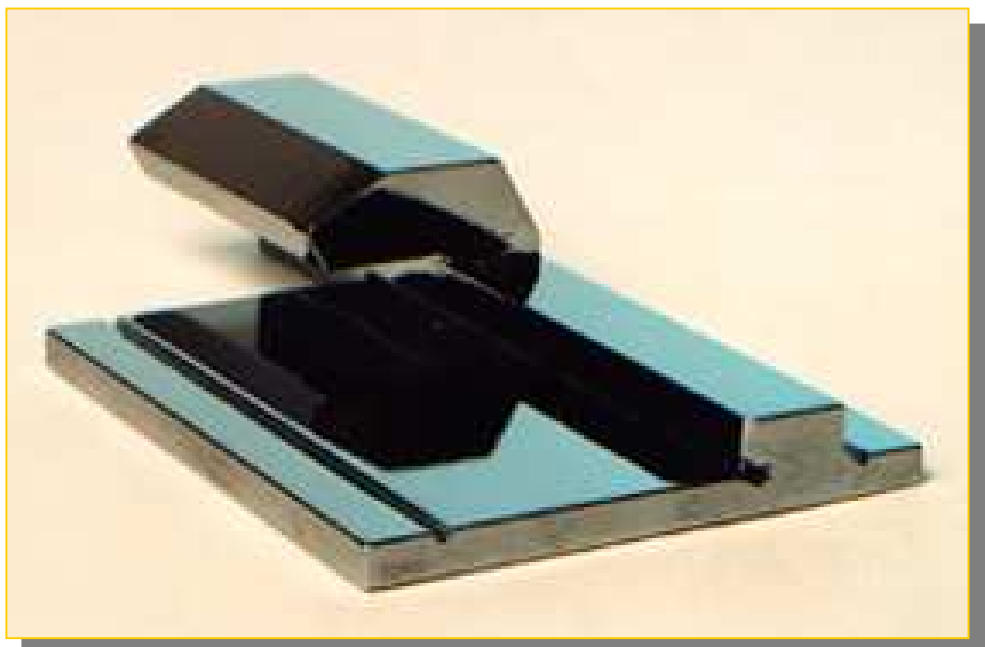
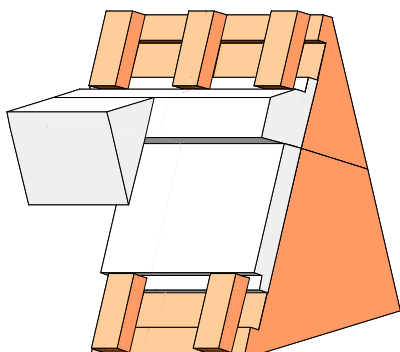


Si(111) inclined channel-cut crystal monochromator designed for the ALOISA beamline.

energy range: 2.8 to 8 KeV

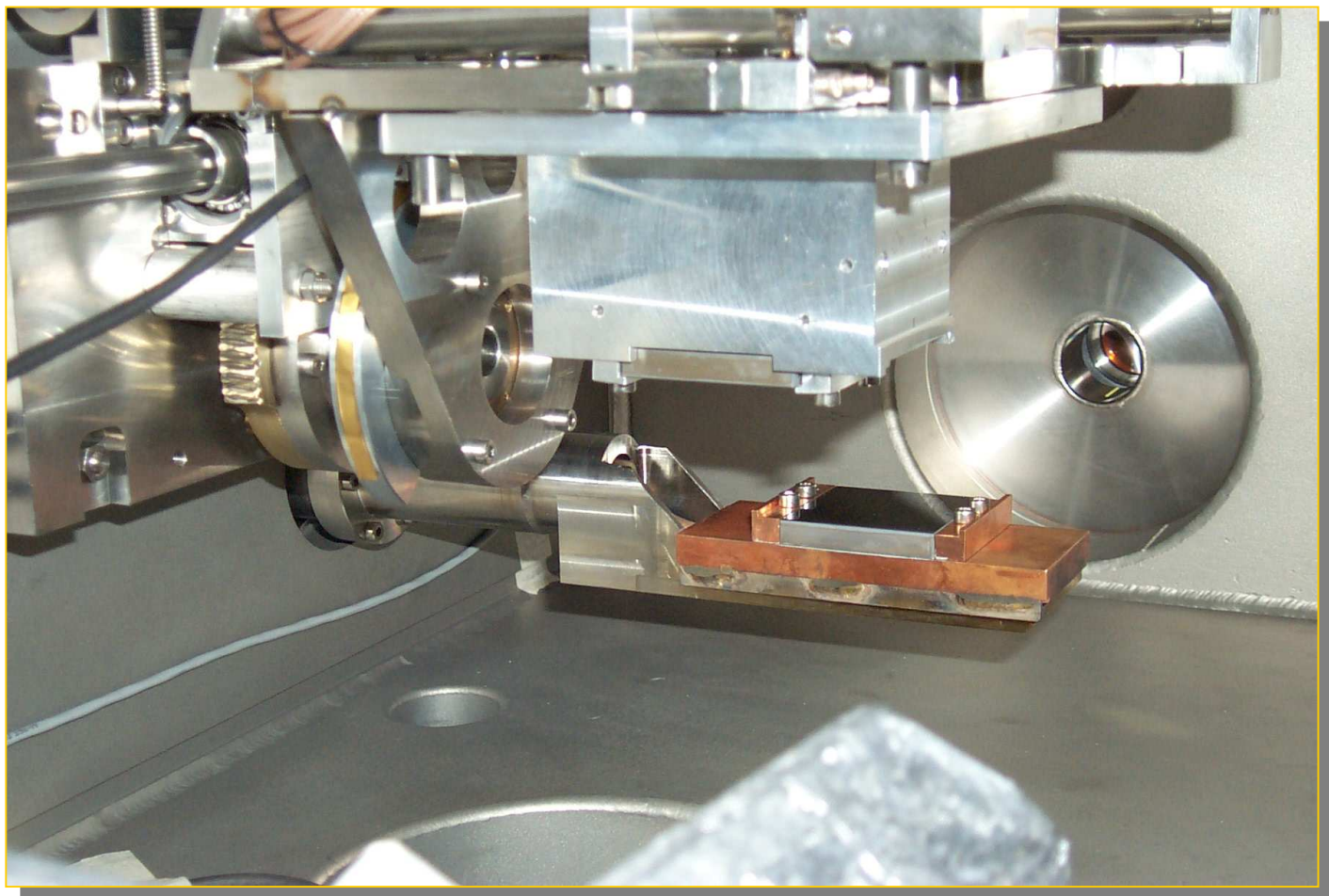
beam dimension: 3x3 mm

source: wiggler-ondulator



E. Busetto et al.: "The High Energy Monochromator for the ALOISA Beamline". Rev. Sci. Instrum. **66** (2), February 1995

A new prototype of monochromator under test with x-rays



*Sincrotrone Trieste S.c.p.A.
Hard-X Ray Optics
Laboratory*

- Detector for Hard X-rays

- Two large families:

single counters
integrators

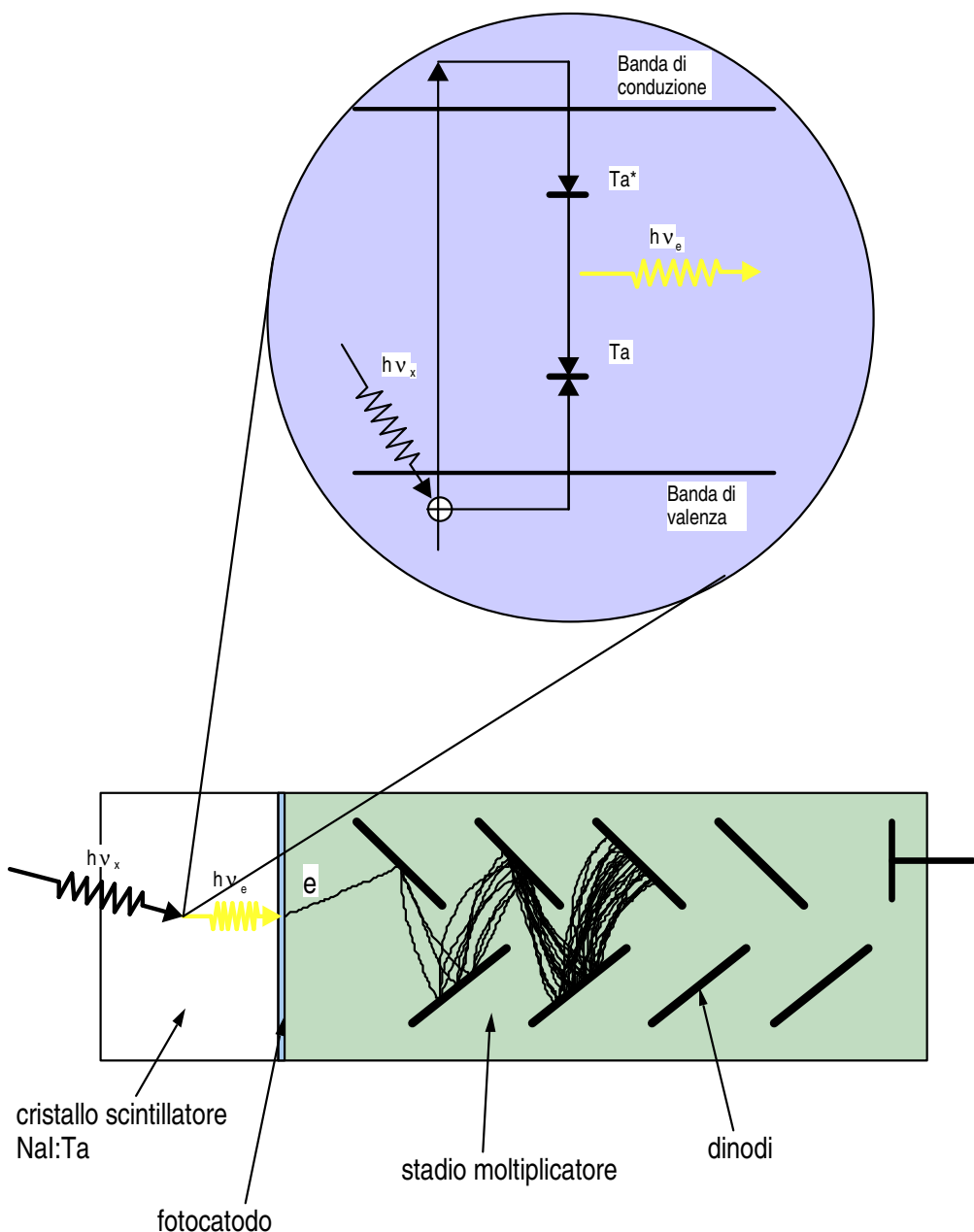


Sincrotrone Trieste S.c.p.A.
Hard-X Ray Optics
Laboratory

- Single counters :
- These systems allow to collect all the electrons produced by the absorption of an x-ray.
- The mean number of electrons produced during the absorption process is proportional to energy of the single x-ray.

Scintillatori

I rivelatori ascintillazione sono il risultato dell'accoppiamento di un cristallo isolante drogato e di un convertitore-moltiplicatore optoelettronico, il fototubo



Integratori

- Sono sistemi di rivelazione “integrata” nel tempo dove si perde la correlazione diretta fra elettroni prodotti ed energia del fotone incidente.
- L'intensità del segnale locale deve essere proporzionale al numero di fotoni assorbiti nella stessa zona.

La pellicola radiografica

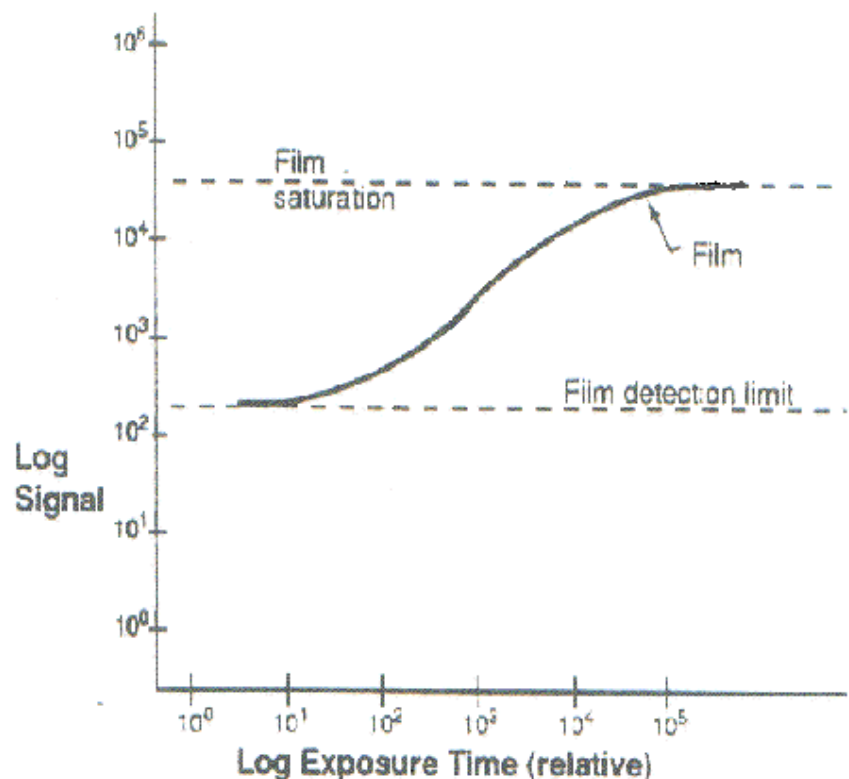
è stato ed è tuttora uno tra i più usati rivelatori ad integrazione sfrutta la sensibilità alle radiazioni elettromagnetiche degli alogenuri di argento in particolare dell' AgBr. La reazione fotochimica produce ioni di Ag^+ con una densità proporzionale alla quantità di radiazione assorbita. Le sostanze fortemente riducenti utilizzate negli sviluppi trasformano Ag^+ , localmente prodotto, in Ag metallico dalla tipica colorazione nera.



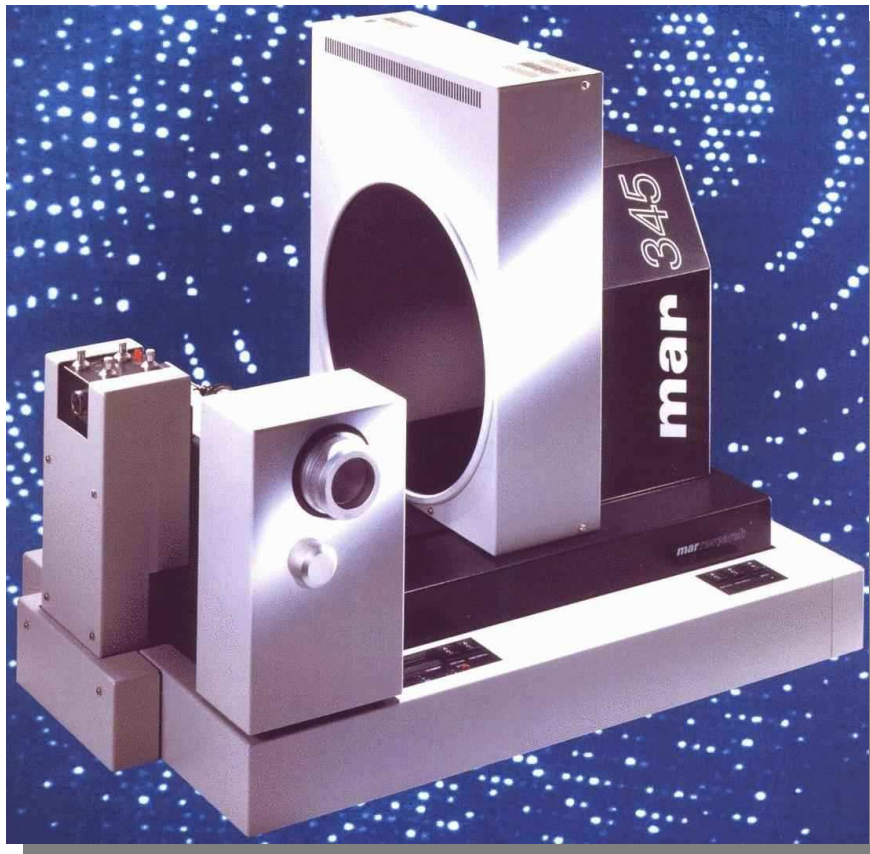
Sincrotrone Trieste S.c.p.A.
Hard-X Ray Optics
Laboratory

Curva caratteristica della densità contro il tempo di esposizione

Linearità e range dinamico delle emulsioni fotografiche

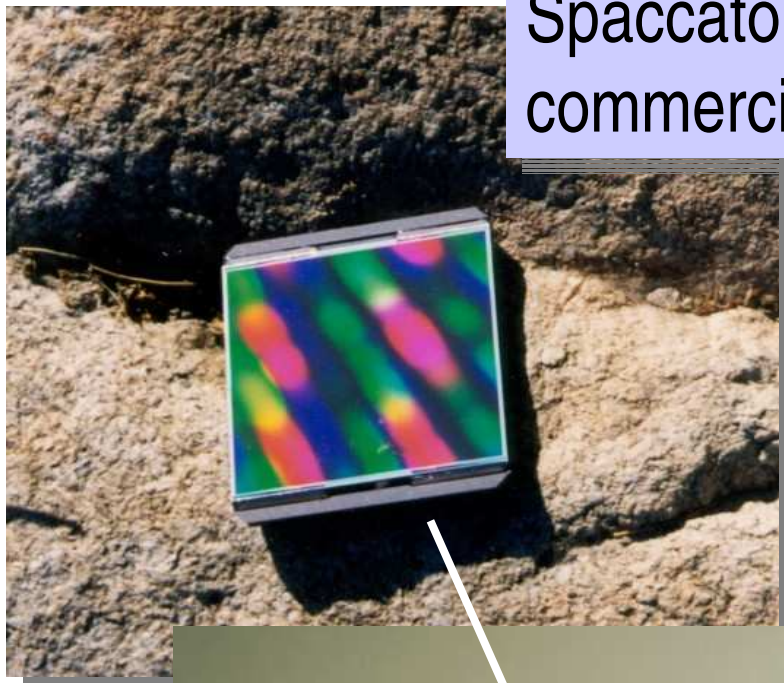


Integratori bidimensionali digitali



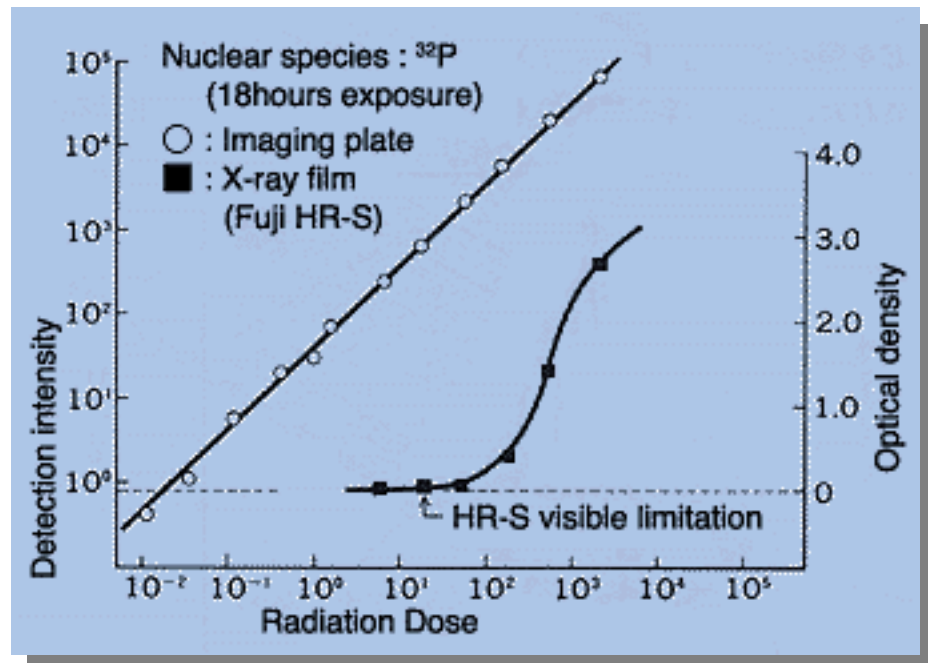
Sincrotrone Trieste S.c.p.A.
Hard-X Ray Optics
Laboratory

Spaccato di un rivelatore CCD commerciale per raggi X

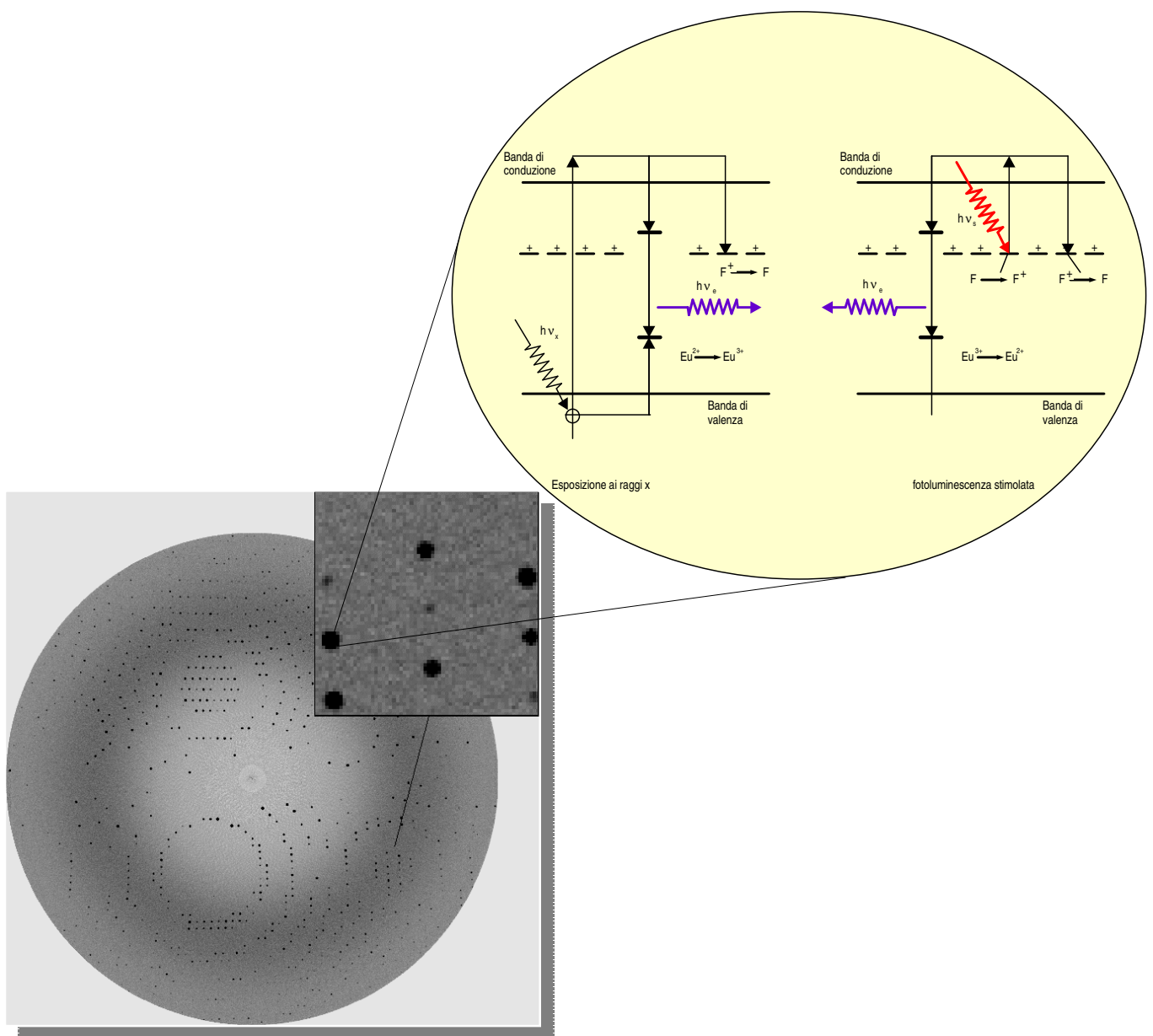


Sincrotrone Trieste S.c.p.A.
Hard-X Ray Optics
Laboratory

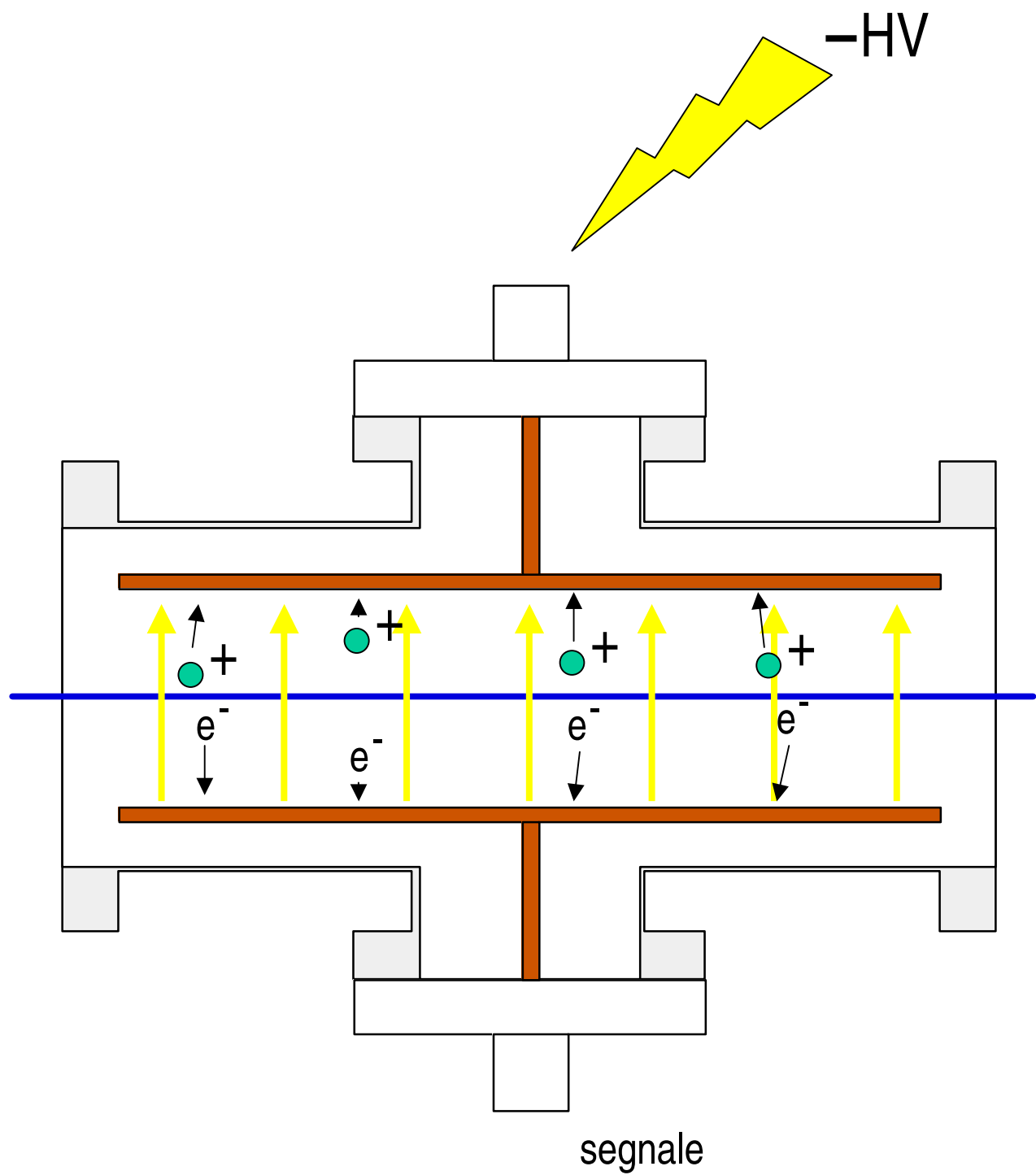
Linearità, range dinamico ed efficienza a confronto



Fisica dell'Image Plate.....un rivelatore analogico a lettura digitale



I rivelatori a gas : principio di funzionamento



Wiggler insertion devices at ELETTRA

Permanent magnet Wiggler W14.0 XRD1 source:

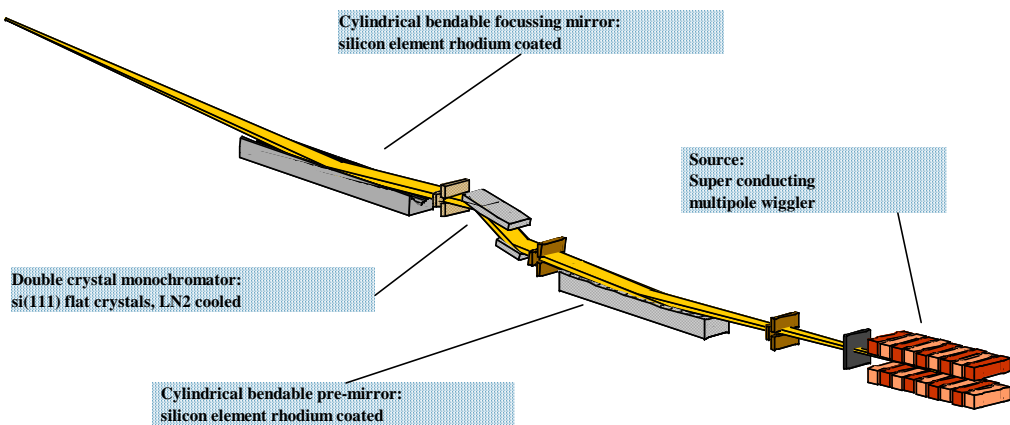
*	B_0	= 1.6 Tesla
*	Period length	= 140 mm
*	No. of poles	= 59
*	Total length	= 4500 mm
*	K_y	= 19.6
*	E_{cm}	= 4.2 Kev (2GeV) / 6.0KeV (2.4GeV)

Multipole Superconducting Wiggler XRD2 source:

*	B_0	= 3.5 Tesla
*	Period length	= 64 mm
*	No. of poles	= 49
*	Total length	= 1568 mm
*	K_y	= 20.9
*	E_{cm}	= 9.2 KeV(2GeV) / 13.2KeV(2.4GeV)

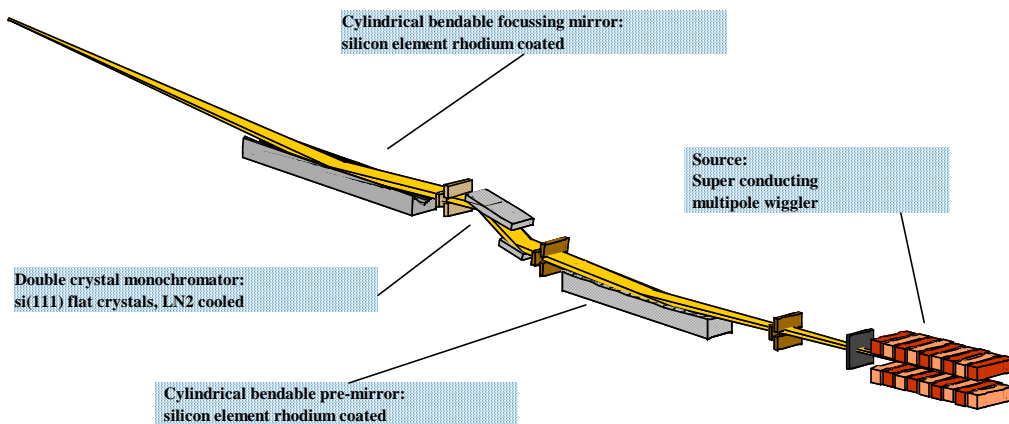


Diffraction2 conceptual layout



Sincrotrone Trieste S.c.p.A.
Hard-X Ray Optics
Laboratory

Diffraction2 conceptual layout



Premirror:

Final shape:

Tangential radius:

Grazing angle:

Source distance:

cylindrical vertical collimator

13.5 Km

0.18° (200 µrad vertical)

21139 mm

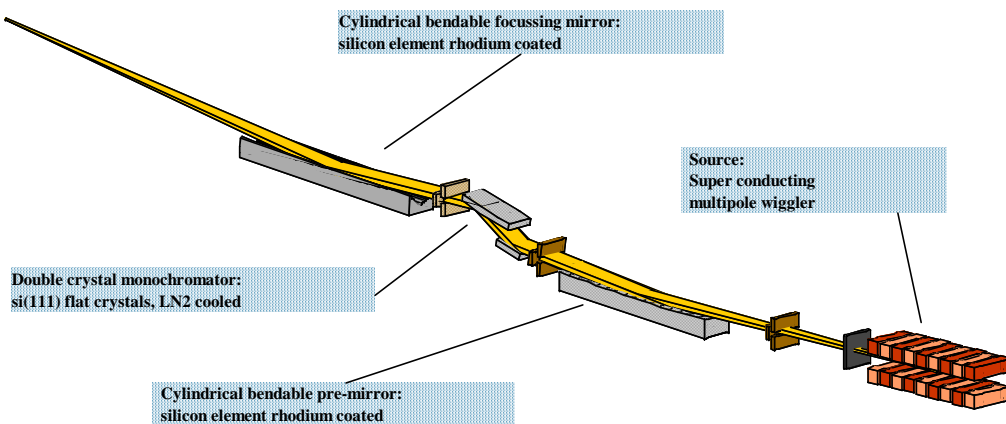
Active optical surface:

1400 x 45 mm²



Sincrotrone Trieste S.c.p.A.
Hard-X Ray Optics
Laboratory

Diffraction2 conceptual layout



Premirror:

Final shape:

Tangential radius:

Grazing angle:

Source distance:

cylindrical vertical collimator

13.5 Km

0.18° (200 μ rad vertical)

21139 mm

Active optical surface:

1400 x 45 mm²

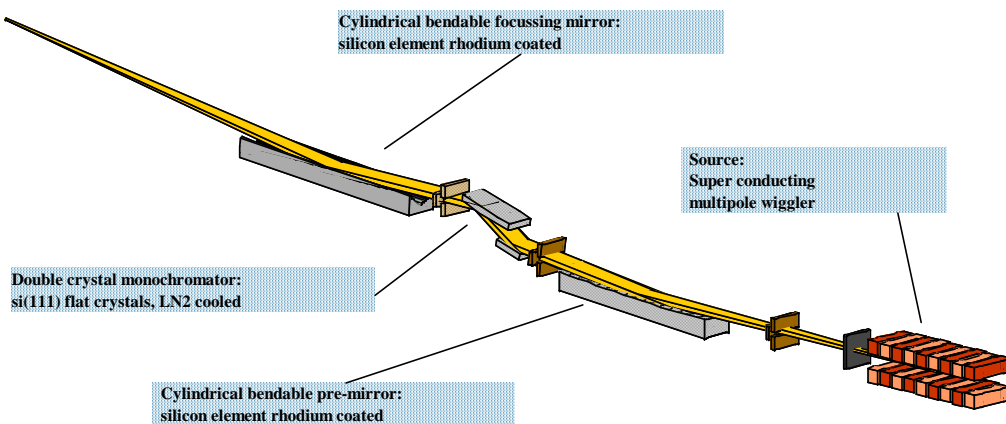
Focalising mirror:

Final shape	toroidal
Tangential radius:	6.0 Km (0.18°)
Saggittal radius:	49.9 mm (0.18°)
Grazing angle:	0.18°
Source distance:	26932 mm
Active optical surface:	1400 x 55 mm ²
Focal distance:	11000 mm with 0.18°
Demagnification:	1.9:1 vertical plane 2.4:1 horizontal plane



Sincrotrone Trieste S.c.p.A.
Hard-X Ray Optics
Laboratory

Diffraction2 conceptual layout



Premirror:

Final shape:

Tangential radius:

cylindrical vertical collimator

13.5 Km

Grazing angle:

0.18° (200 μ rad vertical)

Source distance:

21139 mm

Active optical surface:

1400 x 45 mm²

Focalising mirror:

Final shape
Tangential radius:
Saggittal radius:
Grazing angle:
Source distance:
Active optical surface:
Focal distance:
Demagnification:

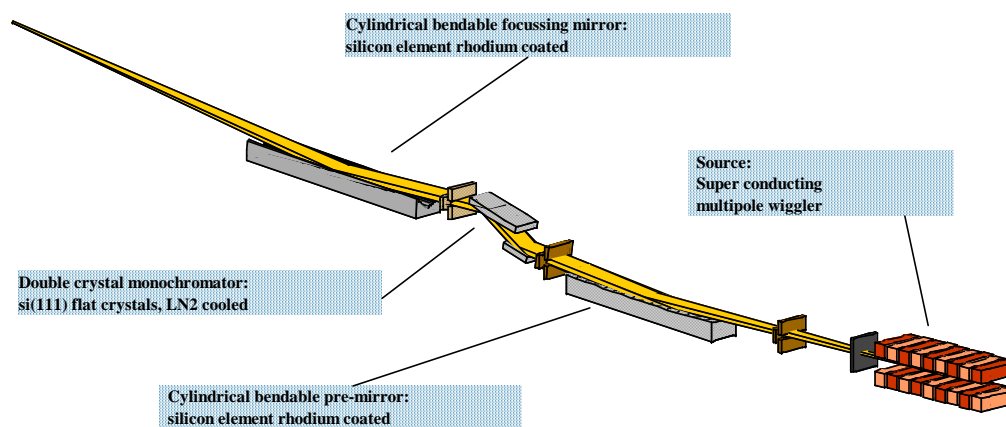
toroidal
6.0 Km (0.18°)
49.9 mm (0.18°)
0.18°
26932 mm
1400 x 55 mm²
11000 mm with 0.18°
1.9:1 vertical plane
2.4:1 horizontal plane

Horizontal acceptance: 1mrad max
Vertical acceptance: 200 μ rad



Sincrotrone Trieste S.c.p.A.
Hard-X Ray Optics
Laboratory

Diffraction2 conceptual layout



Focalising mirror:

Final shape	toroidal
Tangential radius:	6.0 Km (0.18°)
Sagittal radius:	49.9 mm (0.18°)
Grazing angle:	0.18°
Source distance:	26932 mm
Active optical surface:	1400 x 55 mm ²
Focal distance:	11000 mm with 0.18°
Demagnification:	1.9:1 vertical plane 2.4:1 horizontal plane

Horizontal acceptance:
Vertical acceptance:

1mrad max
200 µrad

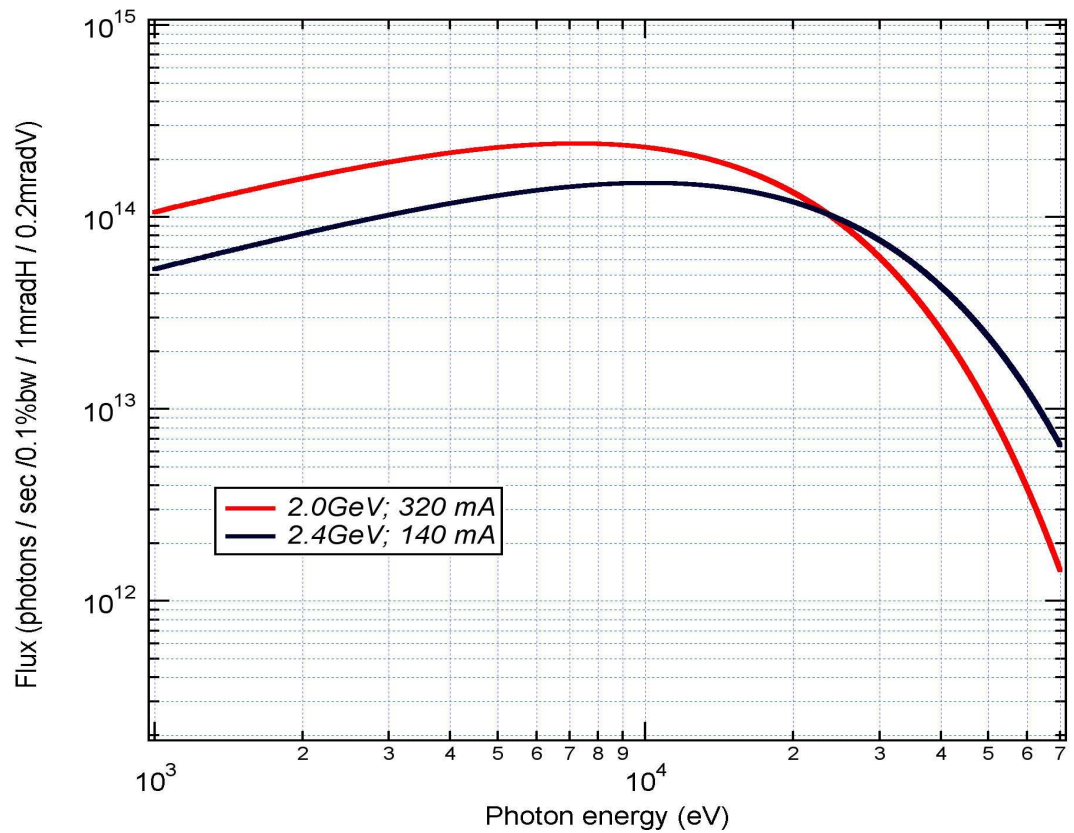


Sincrotrone Trieste S.c.p.A.
Hard-X Ray Optics
Laboratory

Premirror:

Final shape:	cylindrical vertical collimator
Tangential radius:	13.5 Km
Grazing angle:	0.18° (200 µrad vertical)
Source distance:	21139 mm

Active optical surface: 1400 x 45 mm²



wavelength cutoff [Å]
energy cutoff [keV]
grazing angle[deg]



SCW 2GeV, 320 mA, 1 mradH x 0.2mradV

Incoming power [watt]
absorbed power [watt]
reflected power [watt]

mirror setup

	584	664	748
0.5 □ 24.8KeV 0.1505ū	180 404	185 479	190 557
0.55 □ 22.5KeV 0.167ū	213 371	219 446	225 523
0.6 □ 20.7KeV 0.185ū	250 334	257 407	265 483
0.73 □ 17KeV 0.225ū	329 255	339 325	349 398
	1.5 □ 8.3KeV 900μm	2 □ 6.2KeV 360μm	3 □ 4.1KeV 100μm

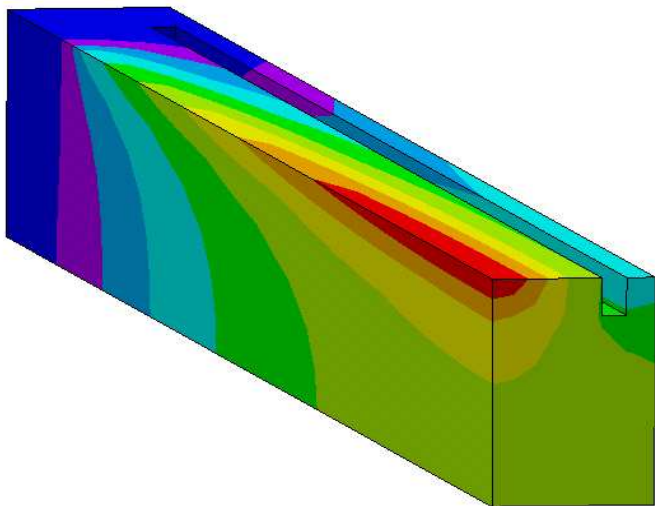


wavelength cutoff [Å]
energy cutoff [keV]
thickness [μm]

Graphite filter setup



Sincrotrone Trieste S.c.p.A.
Hard-X Ray Optics
Laboratory



ANSYS 5.7
NOV 20 2003
10:48:41

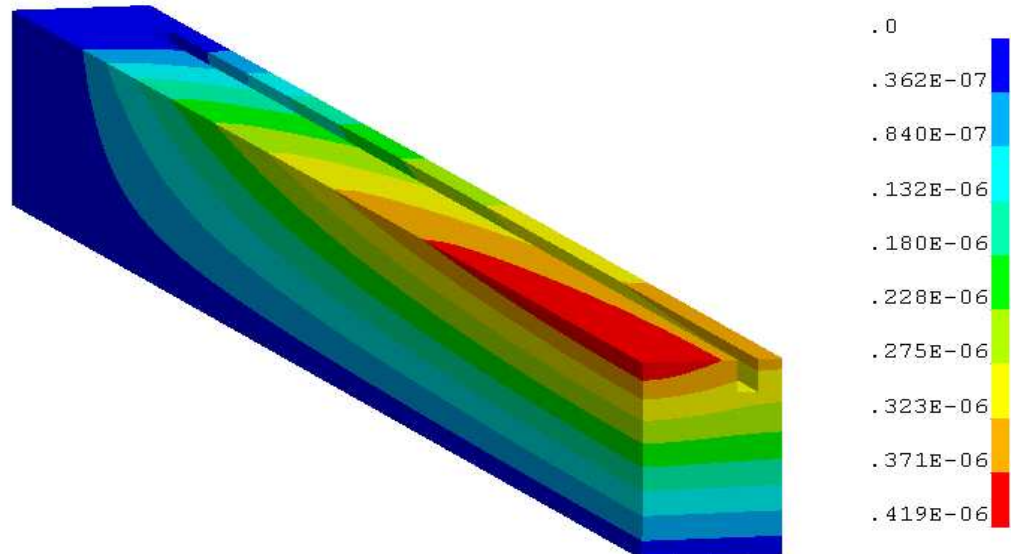
273.64
273.935
274.231
274.526
274.821
275.116
275.411
275.707
276.002
276.297

**case of C-filter 360 μm / 0.185° grazing angle
257 Watt absorbed**

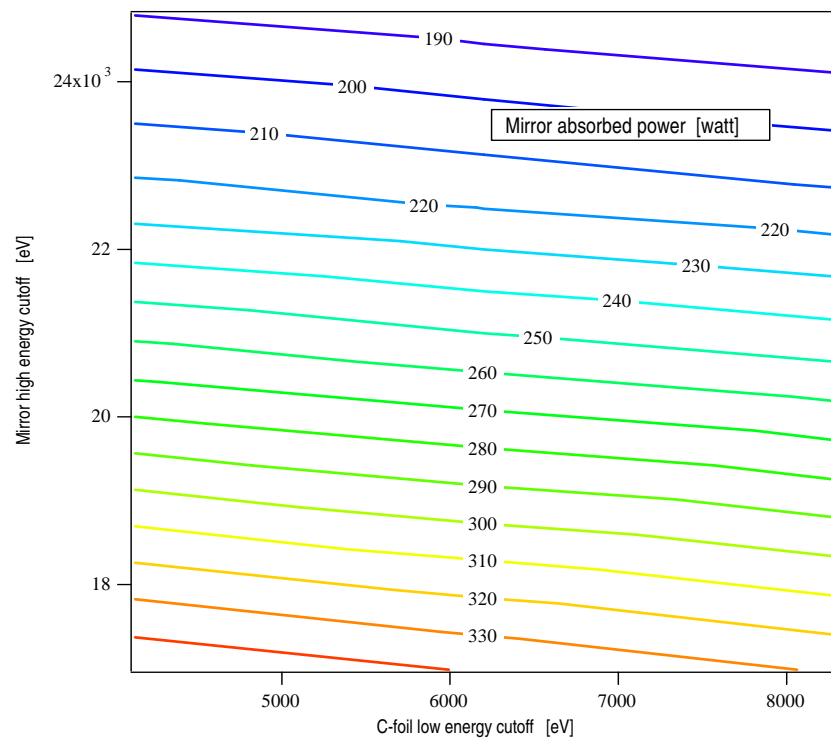
Temperature distribution [K°]



Mirror deformation [m]
The coolant is water at 293K°
and the flow is 300 l/h

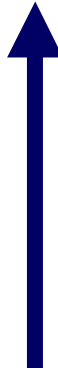


Sincrotrone Trieste S.c.p.A.
Hard-X Ray Optics
Laboratory

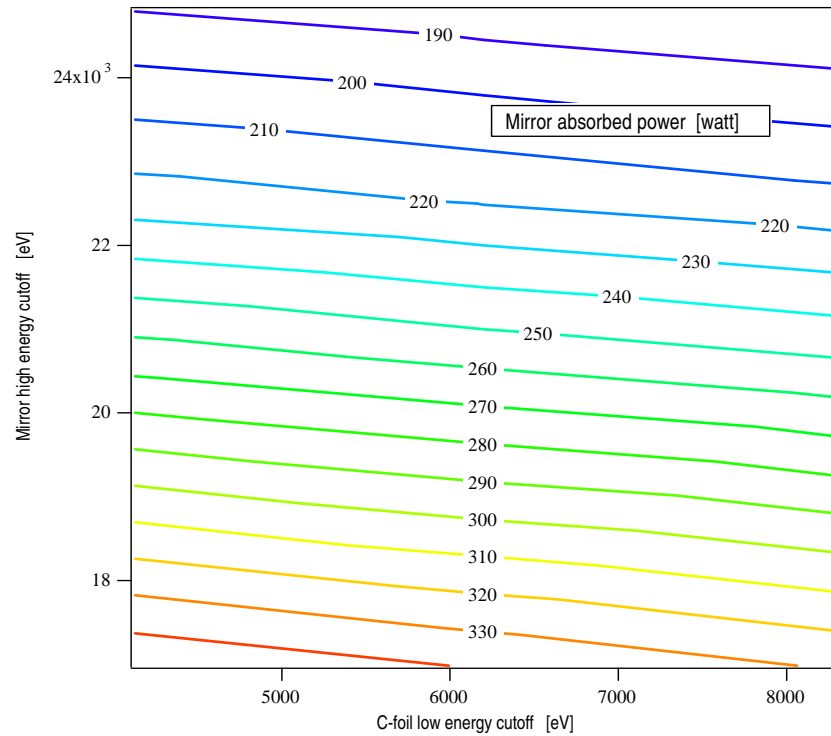


SCW 2GeV, 320 mA, 1 mradH x 0.2mradV

*because of the reflectivity the
the mirror absorbed power depends
on the low-pass filter threshold mostly*

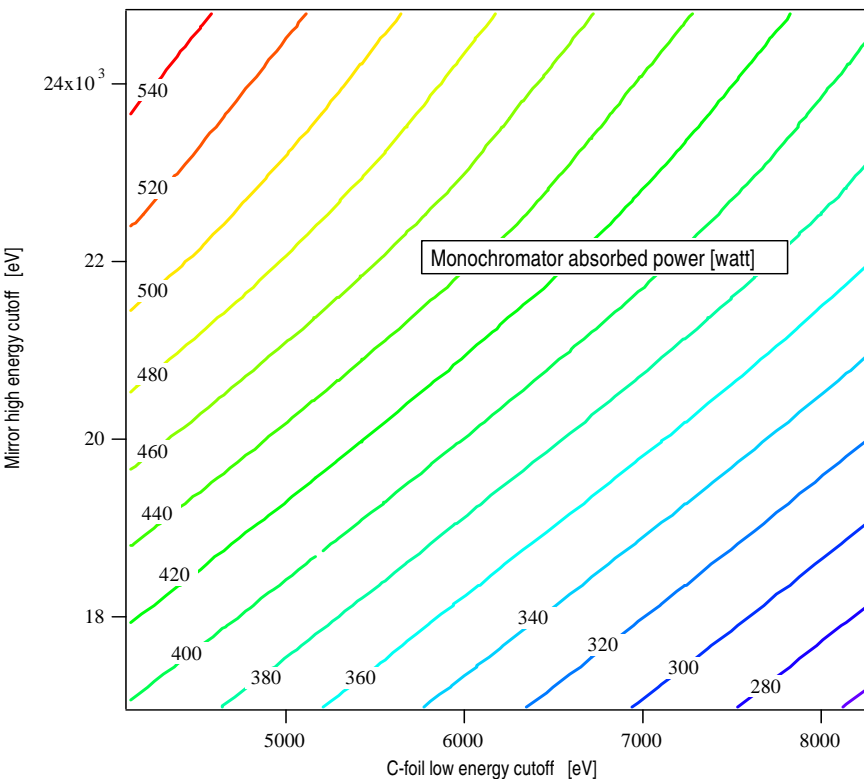


Sincrotrone Trieste S.c.p.A.
Hard-X Ray Optics
Laboratory



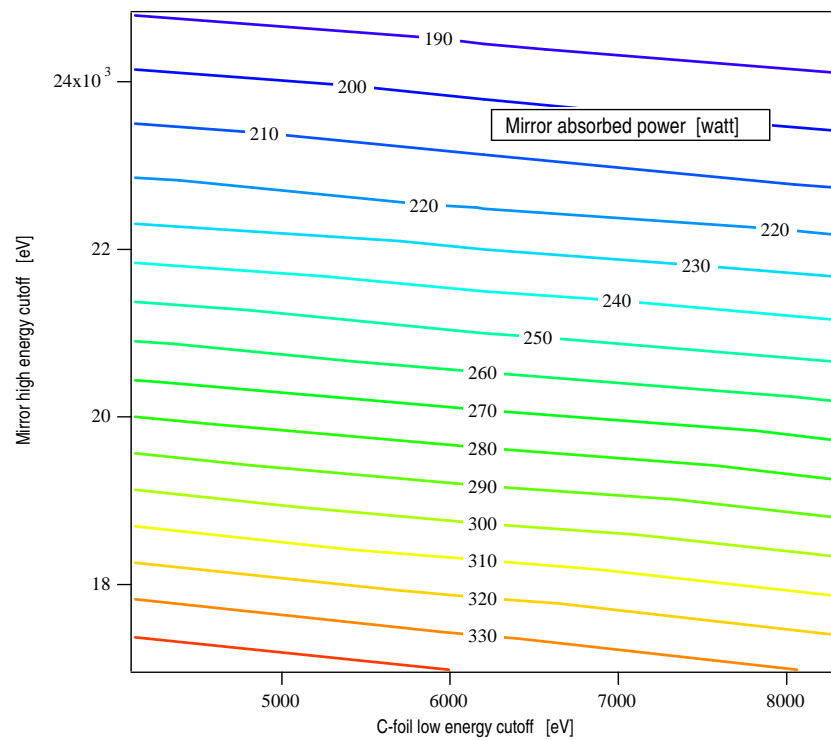
because of the reflectivity the
the mirror absorbed power depends
on the low-pass filter threshold mostly

SCW 2GeV, 320 mA, 1 mradH x 0.2mradV



**the high-pass filter threshold now has a
not negligible contribution**

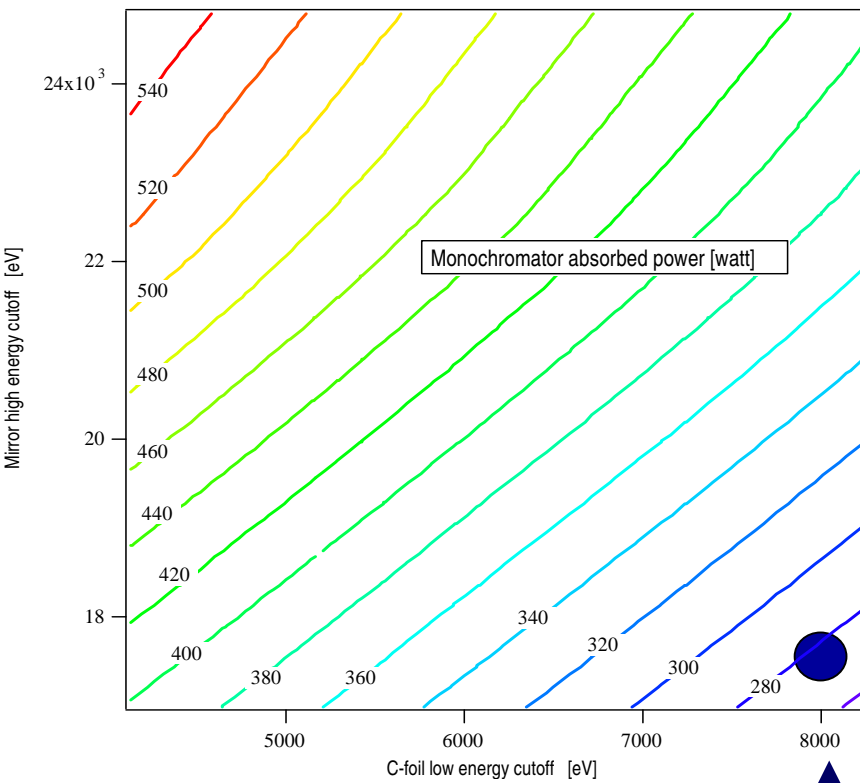




*because of the reflectivity the
the mirror absorbed power depends
on the low-pass filter threshold mostly*

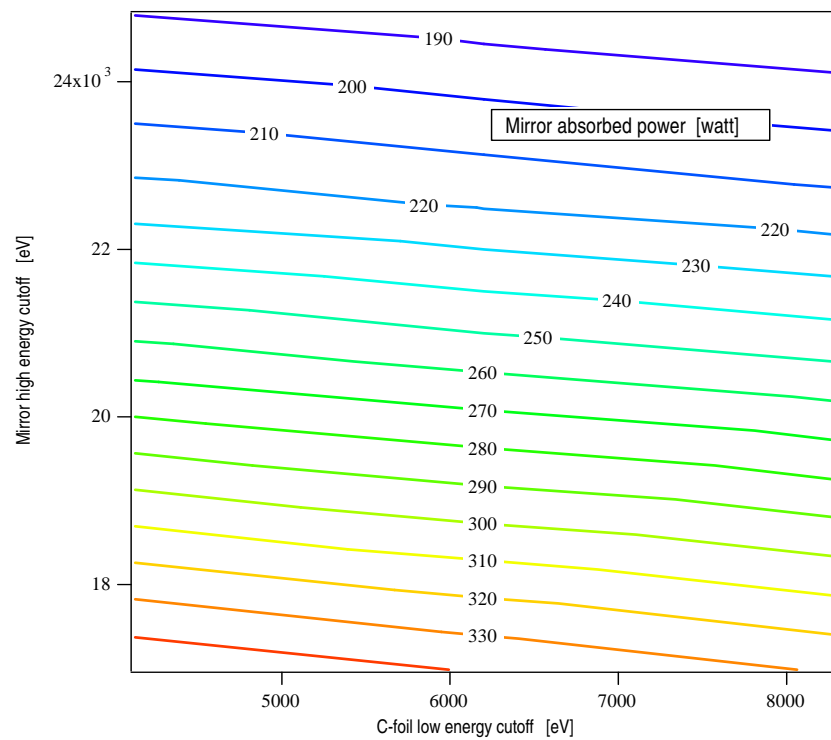


SCW 2GeV, 320 mA, 1 mradH x 0.2mradV



*the high-pass filter threshold now has a
not negligible contribution
first step: H₂O as coolant is still almost ok*

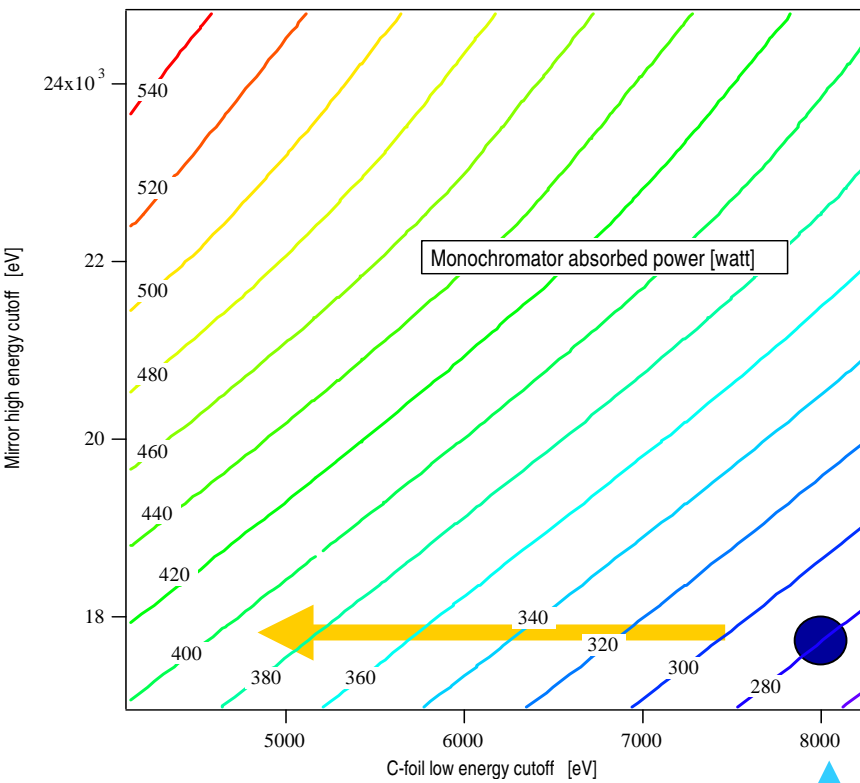




*because of the reflectivity the
the mirror absorbed power depends
on the low-pass filter threshold mostly*

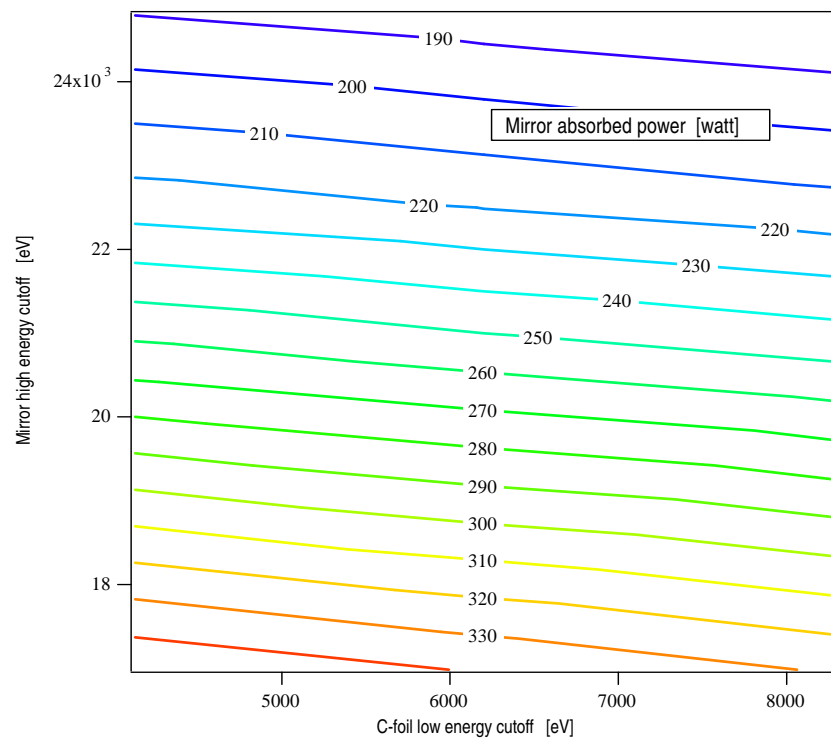


SCW 2GeV, 320 mA, 1 mradH x 0.2mradV



*the high-pass filter threshold now has a
not negligible contribution
first step: H₂O as coolant is still almost ok*

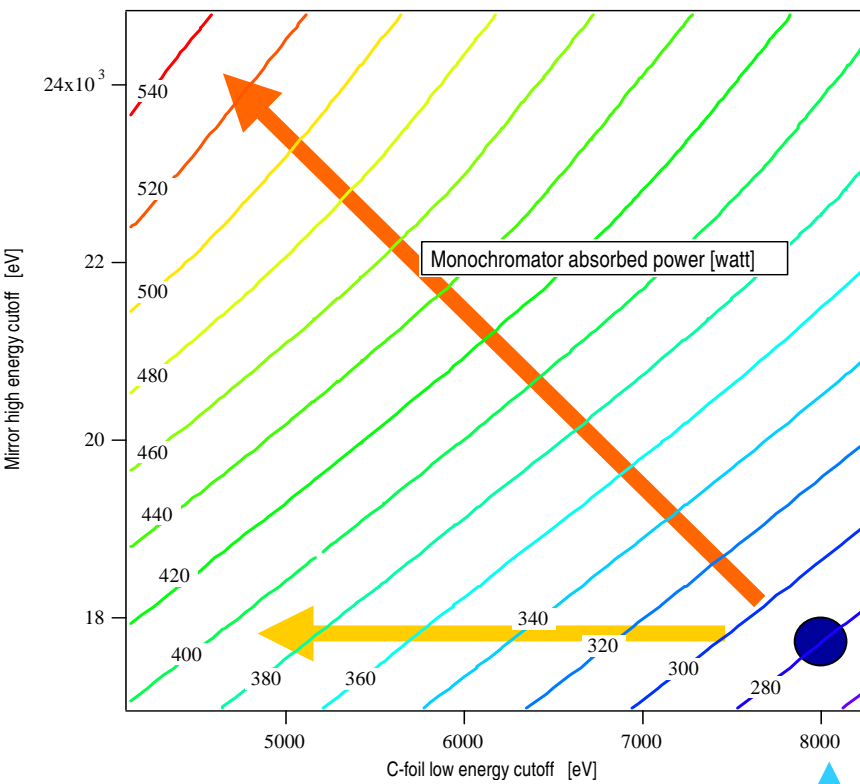
in a second time: extend the range in the low energy direction



*because of the reflectivity the
the mirror absorbed power depends
on the low-pass filter threshold mostly*



SCW 2GeV, 320 mA, 1 mradH x 0.2mradV



*the high-pass filter threshold now has a
not negligible contribution
first step: H₂O as coolant is still almost ok*

*in a second time: extend the range in the low energy direction
or, if requested, open the energy window.....both with LN2 as coolant*